

Impact history of the HED parent body(ies) clarified by new $^{40}\text{Ar}/^{39}\text{Ar}$ analyses of four HED meteorites and one anomalous basaltic achondrite

Trudi Kennedy^{a,*}, Fred Jourdan^b, Alex W.R. Bevan^{a,c,d}, M.A. Mary Gee^a, Adam Frew^b

^a School of Earth and Environment, University of Western Australia, 35 Stirling Hwy, Crawley 6009, Australia

^b Western Australian Argon Isotope Facility, JdL Centre & Applied Geology, Curtin University, GPO Box U1987, Perth, Western Australia 6845, Australia

^c Department of Earth & Planetary Sciences, Western Australian Museum, Locked Bag 49, Welshpool DC, Western Australia 6986, Australia

^d Department of Imaging and Applied Physics, Curtin University, GPO Box U1987, Perth, Western Australia 6845, Australia

Received 16 August 2012; accepted in revised form 28 March 2013; available online 10 April 2013

Abstract

We investigate the thermal/impact histories of four HED meteorites: one cumulate eucrite (Lake Carnegie) two brecciated basaltic eucrites (Camel Donga, Millbillillie), one howardite (Old Homestead 003) and an anomalous basaltic achondrite (Deakin 010). We have measured eight convincing new $^{40}\text{Ar}/^{39}\text{Ar}$ ages for three HED meteorites. Laser incremental $^{40}\text{Ar}/^{39}\text{Ar}$ analyses of carefully separated small grains ($<250\ \mu\text{m}$) of plagioclase, pyroxene, matrix and melt rock from these meteorites yielded well-defined plateau and/or isochron ages for two samples of Lake Carnegie, four samples of Millbillillie and two samples of Camel Donga.

Two concordant $^{40}\text{Ar}/^{39}\text{Ar}$ plateau ages were obtained for plagioclase separates from Lake Carnegie, resulting in a weighted mean age of combined plateau ages of 4507 ± 20 Ma. Millbillillie recorded three impact events at 3722 ± 55 Ma, 3579 ± 28 Ma and 3313 ± 174 Ma from plagioclase, matrix, and pyroxene respectively; this highlights the power of the K/Ar system to record impacts of different magnitudes experienced by a single meteorite. Two aliquots from Camel Donga returned concordant plateau ages interpreted to represent a single significant impact event at 3693 ± 51 Ma. The anomalous basaltic achondrite, Deakin 010, did not yield any plateau and resulted in a series of minimum apparent ages with an oldest minimum age of ≥ 3.66 Ga for the largest impact recorded. Cosmic ray exposure ages yielded apparent $^{38}\text{Ar}_c$ ages ranging from 6 to ≥ 40 Ma.

Two clusters of ages that represent significant impacts into the HED parent body may have been identified. The first high-temperature event is recorded by Lake Carnegie and other unbreciated eucrites at ~ 4.5 Ga and is interpreted as a mega-impact, although it is also possible that this age is recording magmatic crystallisation due to the similarity of published Sm–Nd and Pb–Pb ages. Additionally, from statistically reliable isotopic ages, provided in this study, it appears that the age range of major impact heating events post 4.5 Ga might be more tightly restricted (~ 3.8 – 3.5 Ga) than previously suggested (~ 3.4 – 4.1 Ga), however a larger dataset is required before comparison with the range of the lunar heavy bombardment is justified. If HED are indeed from 4 Vesta, we raise the possibility that the impact at ~ 4.5 Ga might be associated with the formation of the south polar Veneneia basin, whereas an age at ~ 3.7 Ga may represent the formation age of either Veneneia, or the younger Rheasilvia impact structure.

© 2013 Elsevier Ltd. All rights reserved.

* Corresponding author.

E-mail addresses: trudi_kennedy@jinet.net.au, 18104469@student.uwa.edu.au (T. Kennedy).

1. INTRODUCTION

The impact history of the HED (howardite, eucrite, diogenite) parent body provides information that helps elucidate the orbital dynamics operational during the formation of the early Solar System. The HED parent body represents one of the few known differentiated asteroids that remain intact from that early time (Moskovitz et al., 2008); other asteroids that differentiated early have been completely disrupted by impacts or have had their crusts and mantles removed (Burbine et al., 1996), as evidenced by the large number of iron meteorites from asteroidal cores. A comprehensive synthesis of HED meteorite impact ages constrained by $^{40}\text{Ar}/^{39}\text{Ar}$ studies (Bogard, 1995, 2011; Bogard and Garrison, 2003) resulted in the observation that a large number of brecciated eucrites have ages that suggest several large impact heating events occurred on the HED parent body between ~ 4.1 – 3.4 Ga with another cluster at 4.5 Ga. In this study we present new accurate and robust $^{40}\text{Ar}/^{39}\text{Ar}$ age data on isolated plagioclase and pyroxene phases, and matrix with minor melt rock, that significantly improve our knowledge of the impact history of the HED parent body.

The HED meteorites are a complex suite of related crustal mafic and ultramafic igneous rocks originating from the same parent asteroid, commonly thought to be 4 Vesta (McCord et al., 1970; Consolmagno and Drake, 1977; Binzel et al., 1997; Gaffey, 1997), or orbitally related V-type asteroids (Binzel and Xu, 1993; Vilas et al., 2000). However, this source is not universally accepted (e.g., see Cruikshank et al., 1991; Wasson and Chapman, 1996). Moreover, a small number of anomalous basaltic achondrites have oxygen isotope ratios indicating that they formed on a different parent body to that of most HED group meteorites (Yamaguchi et al., 2002; Wiechert et al., 2004; Mittlefehldt, 2005; Lentz et al., 2007; Bland et al., 2009; Scott et al., 2009). Finally, angrites belong to a class of basaltic meteorites with well-defined $\Delta^{17}\text{O}$ trends that are marginally resolvable (Clayton and Mayeda, 1996) from other HED meteorites but with distinct mineralogies (Mittlefehldt et al., 1998). This suggests that these meteorites are from a number of parent bodies with basaltic crusts of a similar size and bulk composition that experienced essentially similar processes under different redox conditions and in different regions of the Solar System.

The HED suite comprises orthopyroxenites (diogenites), plagioclase–pigeonite–augite rocks (cumulate eucrites, partial cumulate eucrites, and basaltic brecciated eucrites), and polymict breccias of predominantly HED materials (howardites, polymict eucrites and polymict diogenites) with occasionally a minor component of chondritic impactor material, (Mittlefehldt et al., 1998). From previous studies based on Rb–Sr, Sm–Nd and Pb–Pb systematics, the estimated age of magmatism for the basaltic eucrites ranges from ~ 4.51 Ga (Tera et al., 1997) to ~ 4.60 Ga (Allègre et al., 1975; Nyquist et al., 1986) with a more precise estimate of their formation age, of 4.548 ± 0.058 Ga (Smoliar, 1993). The timing of mantle fractionation of the HED parent body using the Mn–Cr chronometer anchored to the absolute Pb–Pb age of the angrite LEW 86010 is

$4.564.8 \pm 0.9$ Ma, (Lugmair and Shukolyukov, 1998) and the Pb–Pb ages for three cumulate eucrites, determined by Tera et al. (1997), range from ~ 4.40 to ~ 4.48 Ga.

2. PREVIOUS $^{40}\text{Ar}/^{39}\text{Ar}$ DATING OF EUCRITES

2.1. Filtering and statistical approach

The great majority of basaltic eucrites are fragmental breccias that have undergone varying degrees of metamorphism. Brecciation, mixing, and metamorphism of HED materials are attributed to impact and related heating events (Yamaguchi et al., 1996, 1997; Bogard and Garrison, 2003) dated at between ~ 4.1 and 3.4 Ga based on $^{40}\text{Ar}/^{39}\text{Ar}$ thermochronometry (Bogard, 1995; Bogard and Garrison, 2003). However, as noted in Jourdan (2012), most of the $^{40}\text{Ar}/^{39}\text{Ar}$ results obtained on brecciated and unbrecciated eucrites show significantly perturbed age spectra. These perturbed age spectra may indicate that each of the various mineral and matrix phases contained in a whole rock sample has different diffusion characteristics (e.g., closure temperature) which, as a consequence, have recorded different impact events with various intensities and resulted in a mixture of “ages” that are difficult, if not impossible, to deconvolve or; a series of impacts have successively only partially reset the K/Ar chronometer. Therefore, with such a complex dataset, a crucial question arises: is it better to enhance the counting statistics by taking into account most of the data, no matter how complex they are to interpret, or is it better to focus on only the truly accurate age data even if this means discarding most of the data? Most of the previous studies on HED thermochronology have taken the first approach of trying to extract absolute ages of impact events from complex step-heating $^{40}\text{Ar}/^{39}\text{Ar}$ data. In this study, we chose to explore the alternative option: a clear focus on data accuracy in order to limit potential ‘overinterpretation’.

A review and evaluation of previously published $^{40}\text{Ar}/^{39}\text{Ar}$ ages of brecciated and unbrecciated eucrites was undertaken. Published data (89 analyses of brecciated eucrites and 14 analyses of unbrecciated eucrites) were filtered to retain only those with statistically valid ages. In this work, a statistically valid age means that such ages are based on well-defined plateaus, and to some extent mini-plateaus, as defined by including more than 70% or between 50% and 70% of the total ^{39}Ar released respectively (Electronic Annex 1). A plateau means that contiguous steps in an age spectrum are statistically homogenous, which can be verified using simple χ^2 -based statistical tests (e.g., Mahon, 1996; Baksi, 2007; Jourdan et al., 2009; Jourdan, 2012). In short, statistical filtering allows for the elimination of “noise” created by inaccurate apparent age data resulting in ages that are more likely to be associated to an actual event (e.g., McDougall and Harrison, 1999). For terrestrial objects such as Earth impact craters, this approach tends to diminish the apparent extended duration of a given impact event due to external factors such as alteration, metamorphism, and recrystallization, and rather provides information on the true instantaneous age (Jourdan, 2012). In space, it is the variable effects of multiple impacts that

can obscure the age of a major event. Finally, only the ages produced with standards unlikely to introduce heterogeneity (e.g., Renne et al., 1998; Hb3gr; Jourdan and Renne, 2007) and for which the adopted age is indicated, can be used and recalculated for comparison with the new data presented in this study.

Nevertheless, it is important to emphasise that those age data that did not pass our filter are still important as they provide qualitative information such as maximum or minimum ages for a given event, and can/should be used depending upon the goal of the study. Here, only the well-defined plateau (\pm mini-plateaus) age data will be used in our attempt to precisely characterise the exact ages of major impact events on the HED parent body(ies).

2.1.1. Previous $^{40}\text{Ar}/^{39}\text{Ar}$ results on unbrecciated eucrites

Published apparent ages for 14 unbrecciated eucrite analyses range from 4.506 ± 0.009 Ga (unbrecciated basaltic eucrite PCA 82502) to 3.38 ± 0.03 Ga (unbrecciated cumulate eucrite Serra de Magé) with a concentration of ages around 4.5 Ga interpreted as a single large impact event (Bogard and Garrison, 2003). Although most of the $^{40}\text{Ar}/^{39}\text{Ar}$ age spectra seem to appear as relatively well behaved, close scrutiny reveals that the majority of these $^{40}\text{Ar}/^{39}\text{Ar}$ analyses resulted in discordant step ages that did not define true plateau ages (Electronic Annex 1). Only two analyses exhibiting internally consistent plateau ages passed our filter: EET90020,22 and EET90020,26 (an unbrecciated eucrite; Yamaguchi et al., 2001).

2.1.2. Previous $^{40}\text{Ar}/^{39}\text{Ar}$ results on brecciated eucrites

Published apparent $^{40}\text{Ar}/^{39}\text{Ar}$ ages for 89 brecciated eucrites, (Bogard, 1995 and references therein; Kaneoka et al., 1995; Yamaguchi et al., 1996; Kunz et al., 1997; Nyquist et al., 1997; Yamaguchi et al., 2001; Bogard and Garrison, 2003; Buchanan et al., 2005; Korochantseva et al., 2005), range from 4.5 Ga (Pasamonte polymict eucrite) to 0.35 ± 0.02 Ga (melt separate from ALH81011). Close scrutiny of these $^{40}\text{Ar}/^{39}\text{Ar}$ analyses reveals that they all resulted in discordant step ages that did not define true plateau ages. In our opinion, the virtual absence of robust well-characterized events leaves the true duration of the bombardment of the HED parent body by major asteroids relatively unconstrained.

In this study, the $^{40}\text{Ar}/^{39}\text{Ar}$ technique was applied to five HED meteorites to tentatively obtain information on events such as crystallisation and metamorphic and impact heating that have affected the HED parent body, and in particular to help constrain the true duration of the major bombardment period at the surface of the HED parent body. The five samples range from an unbrecciated, coarse-grained cumulate eucrite (Lake Carnegie) through brecciated basaltic eucrites (Camel Donga, Millbillillie, Deakin 010) to a howardite (Old Homestead 003) (Palme et al., 1988; Yamaguchi et al., 1994; Kennedy et al., unpublished). Sample descriptions are provided in Table 1 and images are in Fig. 1. It is worth noting that Deakin 010 is an anomalous basaltic eucrite with unique O-isotope ratios (Kennedy et al., unpublished), which probably argues for a distinct parent body compared to other HED main group eucrites.

3. METHODOLOGY

3.1. Sample preparation and analysis

Pyroxene, plagioclase and matrix grains, which included minor melt rock components, were selected from each meteorite depending on the individual petrology of the samples. Pyroxene was included as it has been demonstrated (Cassata et al., 2010, 2011) that this mineral has the potential to record information concerning brief, high-temperature, shock heating events experienced by meteorites and their parent bodies, because of the enhanced diffusivity of Ar in pyroxene at high-temperature. Such events most likely correspond to small, localised impacts, in contrast to the larger impacts that generate the relatively high and long-lasting post-impact temperatures necessary to reset the $^{40}\text{Ar}/^{39}\text{Ar}$ system in matrix, glass, and plagioclase phases.

Small pieces (~ 0.05 g) of selected material, excluding fusion crust, were crushed with care and material for analysis was hand-picked under a binocular microscope. Grains of as similar a size (~ 250 μm in diameter) as possible were selected to optimise consistent ^{39}Ar release. Laser incremental heating was conducted on selected aliquots, each with the minimum possible size to ensure maximum sample homogeneity thus enhancing the probability of obtaining plateau ages. Howardite matrix material was also selected from ~ 250 μm sized grains, however it is likely that these grains were not homogeneous matrix due to the potentially mixed nature of a howardite at the 0–5 mm size, but it is unlikely that different clasts were sampled due to the small amount of material available to select grains from. Plagioclase, pyroxene or matrix aliquots were loaded into wells in a 19 mm diameter and 3 mm deep aluminium disc. Samples were not pre-heated; the disc was irradiated for 25 h in the Hamilton McMaster University nuclear reactor (Canada). Upon return from the reactor, multi-grain populations of plagioclase (i.e., ~ 10 grains) or pyroxene (~ 12 –18 grains) were loaded into metal packets made from degassed 0-blank Nb. Matrix, comprising dominantly comminuted pyroxene and plagioclase with minor melt material (or a larger melt component in the case of the howardite), aliquots were analysed as single grains (~ 0.05 mg) directly exposed to the laser.

$^{40}\text{Ar}/^{39}\text{Ar}$ analysis was undertaken at the Western Australian Argon Isotope Facility, at Curtin University, Perth. A blank was analysed for every three to four incremental heating steps and typical ^{40}Ar blanks range from 1×10^{-16} to 2×10^{-16} mol. Step-heating of the samples was carried out using a 110 W Spectron Laser Systems Nd: YAG laser (1064 nm), which was continuously rastered over the sample for 1 min to ensure a homogenously distributed temperature. The resulting isotopic ratios were acquired with the Argus program written by M.O. McWilliams and run within the LabView environment. The raw data (Electronic Annex 2) were processed using the ArArCALC software (Koppers, 2002). The mean J -value (a proxy for neutron fluence values necessary to activate ^{39}K in ^{39}Ar ; McDougall and Harrison, 1999) computed from standard grains within the wells in the aluminium disc sample holder ranges from 0.01000 ± 0.000050 to

Table 1
Sample descriptions and degree of disruption after crystallisation.

Sample name	Sample #	Classification	Description	Degree of disruption	Material selected
Camel Donga	WAM13715	Brecciated basaltic eucrite	Crystal and lithic fragments in a comminuted silicate matrix (Fig. 1) and is distinctive from other eucrites in that it contains a high metallic iron content of ~2% ^a	Brecciated	Matrix including pyroxene fragments
Millbillillie	WAM13357.3	Brecciated basaltic eucrite	Fine- and coarse-grained clasts in a matrix of comminuted pyroxene and plagioclase (Fig. 2) ^b	Brecciated	Clear & cloudy plagioclase, matrix and very small pyroxene grains
Lake Carnegie	WAM14220	Cumulate eucrite	Pigeonite, orthopyroxene inverted from pigeonite, calcic plagioclase with minor ilmenite, chromite and troilite and very minor Fe-Ni metal (Fig. 3) ^c	Unbrecciated	Clear & cloudy plagioclase, and pyroxene (clino- & ortho)
Deakin 010	WAM14774	Brecciated anomalous basaltic eucrite	Monomict eucrite of coarse- to medium-grained clasts of low-Ca pyroxene and plagioclase with minor ilmenite, chromite, troilite and Fe-Ni metal in a matrix of comminuted pyroxene and plagioclase (Fig. 4) ^c	Brecciated	Cloudy plagioclase and matrix*
Old Homestead 003	WAM15257	Howardite	Lithic clasts including eucrite fragments (some showing ophitic texture) with a minor diogenite component in a clastic, welded, melt matrix of comminuted mineral fragments, and glass (Figs. 5 and 6). Lithic fragments include abundant pyroxene and maskelynite; other minerals include olivine, chromite, ilmenite and Fe-Ni metal ^c	Highly comminuted and brecciated and includes melt material. Plagioclase is converted to maskelynite	Matrix

^a Palme et al. (1988).

^b Yamaguchi et al. (1994) also noted clasts of granulitic breccia and impact melts.

^c (Kennedy et al. unpubl.).

* Note: material selected from WAM14774 was not as homogeneous as that from sample WAM14220, due to its comminuted nature. Plagioclase commonly contains very small amounts of pyroxene and larger pyroxene grains could not be completely separated from plagioclase due to its very small grain size.

0.01012 ± 0.000015 . Mass discrimination was monitored using an automatic air pipette and provided mean values ranging from 1.005199 ± 0.000023 to 1.006532 ± 0.000032 per dalton (atomic mass unit).

The ages were calculated using the decay constants recommended by Renne et al. (2010) calibrated against the U/Pb chronometer. Utilising this new ^{40}K decay constant (Renne et al., 2010), calculated ages are 0.6% older than those obtained using the previous decay constant (Steiger and Jäger, 1977), for instance early Solar System ages calculated with the new ^{40}K decay constant are older by approximately 15 Ma. Criteria for the determination of plateau are as follows: (1) plateaus must include at least 70% of ^{39}Ar ; (2) the plateau should be distributed over a minimum of 3 consecutive steps agreeing at 95% confidence level and satisfying a probability of fit (P) of at least 0.05. The use of these criteria means that possible perturbed spectra are not used. Plateau ages are given at the 2σ level and are calculated using the mean of all the plateau steps, each weighted by the inverse variance of their individual analytical error. Mini-plateaus are defined similarly except that they include between 50% and 70% of ^{39}Ar . All uncertain-

ties are included in the calculation of the plateau ages and resulting weighted mean age.

3.2. Correction for cosmic ray production and trapped argon

The old apparent ages obtained for these grains also contain information of their journey through space before arrival on Earth, as the grains are likely to have retained their cosmogenic Ar (mostly ^{38}Ar and ^{36}Ar). To enable calculation of an isochron, cosmogenic Ar ($^{36}\text{Ar}_c$) must be subtracted from the total ^{36}Ar . This is achieved by using the cosmogenic standard $^{36}\text{Ar}/^{38}\text{Ar}$ ratio used for Fe- and Ti-poor samples (0.65; for example see details in Korochantseva et al., 2005). The result of this calculation is a $^{40}\text{Ar}/^{36}\text{Ar}$ intercept that consists entirely of trapped Ar and diminishes the scatter of the isochron by removing an extra reservoir of ^{36}Ar , thus leaving only trapped ^{40}Ar and radiogenic Ar in the inverse isochron. However, this approach is only valid if $^{38}\text{Ar}_{\text{CI}}$ (induced from chlorine during reactor irradiation; McDougall and Harrison, 1999) is not present in the sample, which seems to be the case with samples Camel Donga, Millbillillie, Lake Carnegie, Deakin

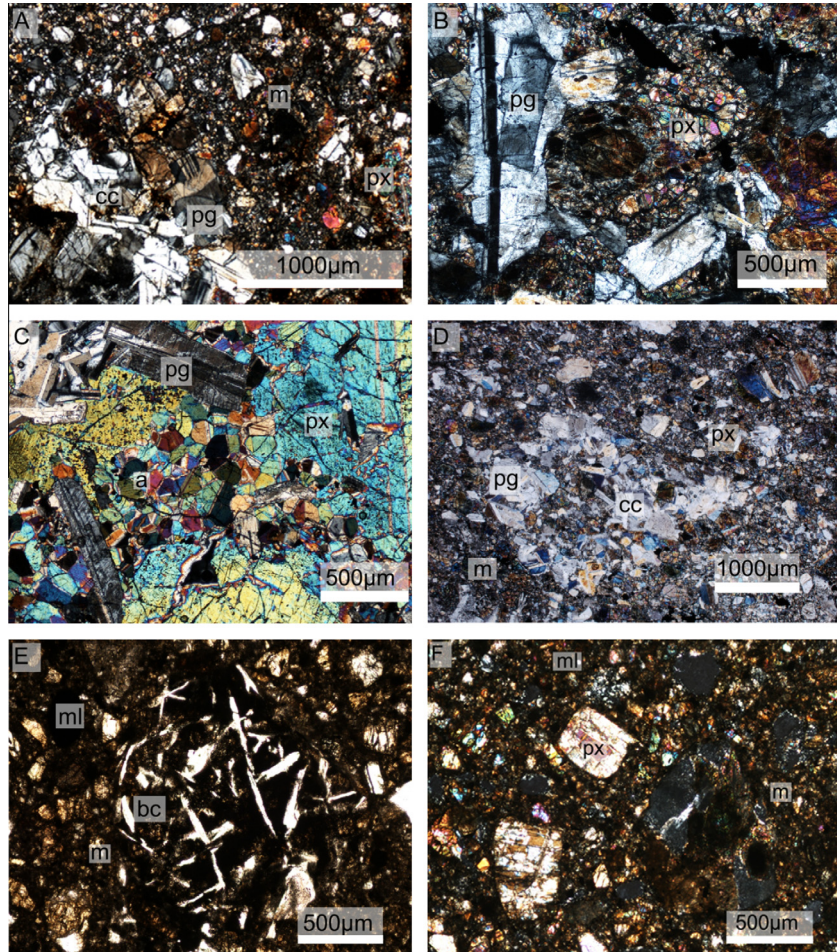


Fig. 1. Microscopy images. Photomicrographs of meteorite sample thin sections. (A) Camel Donga; coarse-grained clast in comminuted matrix; (B) Millbillillie; clast with sub-ophitic texture; (C) Lake Carnegie; coarse-grained cumulate eucrite with annealing texture; (D) Deakin 010 coarse-grained clast (c) in comminuted matrix (m); (E) Old Homestead 003; basaltic clast with plagioclase converted to maskelynite; (F) Old Homestead 003; crystal fragments in matrix (m) of comminuted grains and melt. Abbreviations: a = annealing texture, bc = basaltic clast, cc = coarse-grained clast, m = matrix, ml = melt, pg = plagioclase, px = pyroxene.

010 and Old Homestead 003 where $^{36}\text{Ar}/^{38}\text{Ar}$ is greater than 0.65.

All ages (isochron and plateau) presented in this paper were calculated using the $^{40}\text{Ar}/^{36}\text{Ar}$ trapped ratio obtained by the inverse isochron plot on the same sample. Uncertainties on the initial ratio were propagated in the final calculation.

3.3. Calculation of exposure ages

Cosmic ray exposure (CRE) ages were calculated based on the spallation of Ca to ^{38}Ar due to the interaction of cosmic rays with the sample. To determine the amount of ^{38}Ar in the sample per gram of Ca (see Hennessy and Turner, 1980 for derivation), the following Eq. (1) is used:

$$\frac{^{38}\text{Ar}}{\text{Ca}} = 1.13 \times \frac{^{38}\text{Ar}}{^{37}\text{Ar}} \times \alpha \times J \times 7.012 \times 10^{-3} \quad (1)$$

where

1.13 relates the $^{38}\text{Ar}/^{37}\text{Ar}$ ratio to the cosmogenic-only component.

α = a proportionality factor needed to convert $^{38}\text{Ar}/^{37}\text{Ar}$ into $^{38}\text{Ar}/\text{Ca}$ (Eq. (2))

J = J factor

7.012×10^{-3} = constants of K-decay and unit conversion from $^{38}\text{Ar}/\text{Ca}$ into cc STP/g

$$\alpha = \left(\frac{\text{K}}{\text{Ca}} \right) \div \left(\frac{^{39}\text{Ar}^*}{^{37}\text{Ar}} \right) \quad (2)$$

where

$^{39}\text{Ar}^*$ and ^{37}Ar are produced by neutron activation in the reactor from K and Ca respectively.

To obtain the $^{38}\text{Ar}/^{37}\text{Ar}$ ratio of the sample, isotope correlation diagrams with $^{38}\text{Ar}/^{36}\text{Ar}$ vs. $^{37}\text{Ar}/^{36}\text{Ar}$ (with uncertainties fully propagated) were used (Levine et al., 2007). This allows identification and removal of Ar sources unrelated to the CRE ages, such as solar wind and implanted and adsorbed atmospheric Ar (Niemeyer and Leich, 1976). The $^{38}\text{Ar}/^{37}\text{Ar}$ ratio can then be determined using a regression through the remaining steps satisfying the same statistical conditions described for the inverse isochrons (i.e., a CRE age analysis should have a

P-value > 0.05 to be considered statistically valid) and is converted into the $^{38}\text{Ar}/\text{Ca}$ ratio of the sample by comparison with the Hb3gr standard. The exposure age is calculated assuming a nominal production rate of ^{38}Ar from spallation of Ca of $1.81 \times 10^{-8} \text{ cm}^3 \text{ STP } ^{38}\text{Ar}/\text{gram}$ of Ca/Ma for plagioclase, $2.30 \times 10^{-8} \text{ cm}^3 \text{ STP } ^{38}\text{Ar}/\text{gram}$ of Ca/Ma for pyroxene and a half-way value of $2.05 \times 10^{-8} \text{ cm}^3 \text{ STP } ^{38}\text{Ar}/\text{gram}$ of Ca/Ma for matrix which comprises similar quantities of comminuted plagioclase and pyroxene (Eugster and Michel, 1995; Korochantskaya et al., 2005). As a proportion of the ^{38}Ar will likely arise from Fe and K, and is unaccounted for, the CRE calculations in this study therefore provide maximum ages that, at worst will be too high by up to ~10%, for example if the meteorites are abundantly rich in K or Fe (cf. discussion about the cosmochron approach by Levine et al., 2007).

4. RESULTS

All ages are reported at 2σ . Calculated $^{40}\text{Ar}/^{39}\text{Ar}$ ages are summarized in Table 2 and the plateau age plots are shown in Figs. 2–6. CRE ages are included in the discussion

for each sample, however it should be noted that they reflect an approximate time over which the samples have been bombarded by cosmic rays. During this time period a number of factors could all influence the CRE, including; depth of burial within the original meteoroid, composition, and degree of shielding from cosmic rays, for instance a meteorite from within a larger meteoroid would have been completely shielded before its release by further impacts and may have been partially shielded during its transit time before its fall on Earth. In other words, the CRE age represents a binary mixture between the meteoroid transit time in space following its ejection impact and the exposure age at the surface of the parent body. If the sample was completely shielded at the surface of the parent body, then the CRE ages measured include only the transit time component. In addition, it should be noted that depending upon the degree of shielding (i.e., different depths), the CRE clock will tick at different rates and the CRE ages will consist of a mixture of different time rates. As such, CRE ages always represent a minimum age. The CRE ages are summarised in Table 3 and all cosmochron graphs not included in Fig. 7 are in Electronic Annex 3.

Table 2

Summary of $^{40}\text{Ar}/^{39}\text{Ar}$ ages for three eucrites, one howardite and one anomalous basaltic achondrite.

Sample name	Sample # prefix: WAM	Description	Package or grain	Weighted plateau (Ma)	MSWD	<i>P</i>	% ^{39}Ar	Inverse isochron Ma	MSWD	<i>P</i>	$^{40}\text{Ar}/^{36}\text{Ar}$
Camel	13715-sg1	m	sg	3704 ± 79	0.22	0.99	99.1	3706 ± 97	0.26	0.97	275.2 ± 42.0
Donga	13715-sg2	m	sg	3670 ± 80	0.81	0.63	100	3685 ± 85	0.92	0.51	263.3 ± 12.3
	13715-combo	m	sg1 & sg2	3693 ± 51	0.57	0.93	99.44	3703 ± 59	0.57	0.93	264.9 ± 11.8
Millbillillie	13357.3-plg	Clean plag	p (10 grains)	3722 ± 55	0.67	0.78	70.81	3728 ± 74	0.74	0.7	306.2 ± 13.7
	13357.3-pyx	pyx	p (12 grains)	—	—	—	—	—	—	—	—
	13357.3-pyx + matrix	pyx and m	p (8 grains)	3313 ± 174	0.76	0.72	100	3395 ± 281	0.85	0.61	290.7 ± 20.3
	13357.3-sg1	m	sg	$3413 \pm 73^*$	1.3	0.13	100	—	—	—	-76.5 ± 232.6
	13357.3-sg2	m	sg	3579 ± 28	1.3	0.12	88.73	3579 ± 56	1.37	0.09	309.6 ± 38.3
Lake Carnegie	14220-plg	Cloudy plag	p (7 grains)	4532 ± 32	0.74	0.77	100	4536 ± 51	0.74	0.77	258.7 ± 19.0
	14220-plg	Clear plag	p (7 grains)	4491 ± 26	0.53	0.93	95.93	4493 ± 62	0.59	0.89	230.3 ± 43.8
	14220-plg	Clear and cloudy plag	Combined	4507 ± 20	0.81	0.79	96.77	4489 ± 32	0.91	0.62	276.4 ± 16.0
	14220-pyx	pyx	p (18 grains)	—	—	—	—	—	—	—	—
Deakin 010	14774-plg_1	plag	p (10 grains)	—	—	—	—	—	—	—	—
	14774-sg1	m	sg	$3351 \pm 65(?)$	0.76	0.65	61	3356 ± 89	0.91	0.51	160.1 ± 53.8
	14774-sg5	m	sg	$\geq 3.7 \text{ Ga}$	—	—	—	—	—	—	—
	14774-sg6	m	sg	$3482 \pm 36(?)$	1.4	0.1	63.47	—	—	—	—
Old Homestead	15257-sg1	m	sg	$\geq 3.1 \text{ Ga}$	—	—	—	—	—	—	—
	15257-sg2	m	sg	$\geq 3.6 \text{ Ga}$	—	—	—	—	—	—	—
003	15257-sg3	m	sg	$\geq 3.7 \text{ Ga}$	—	—	—	—	—	—	—

Abbreviations: plag = plagioclase, pyx = pyroxene, m = matrix, p = package (between 7–18 grains loaded into metal packets made from degassed 0-blank Nb), sg = single grain, bold type = robust age, MSWD = mean square weighted deviation and “*P*” = probability.

* $^{40}\text{Ar}/^{36}\text{Ar}$ of sg2 used in the plateau calculation; note that the effect of the choice of the intercept is negligible within error as the data cluster near the radiogenic axis of the inverse isochron.

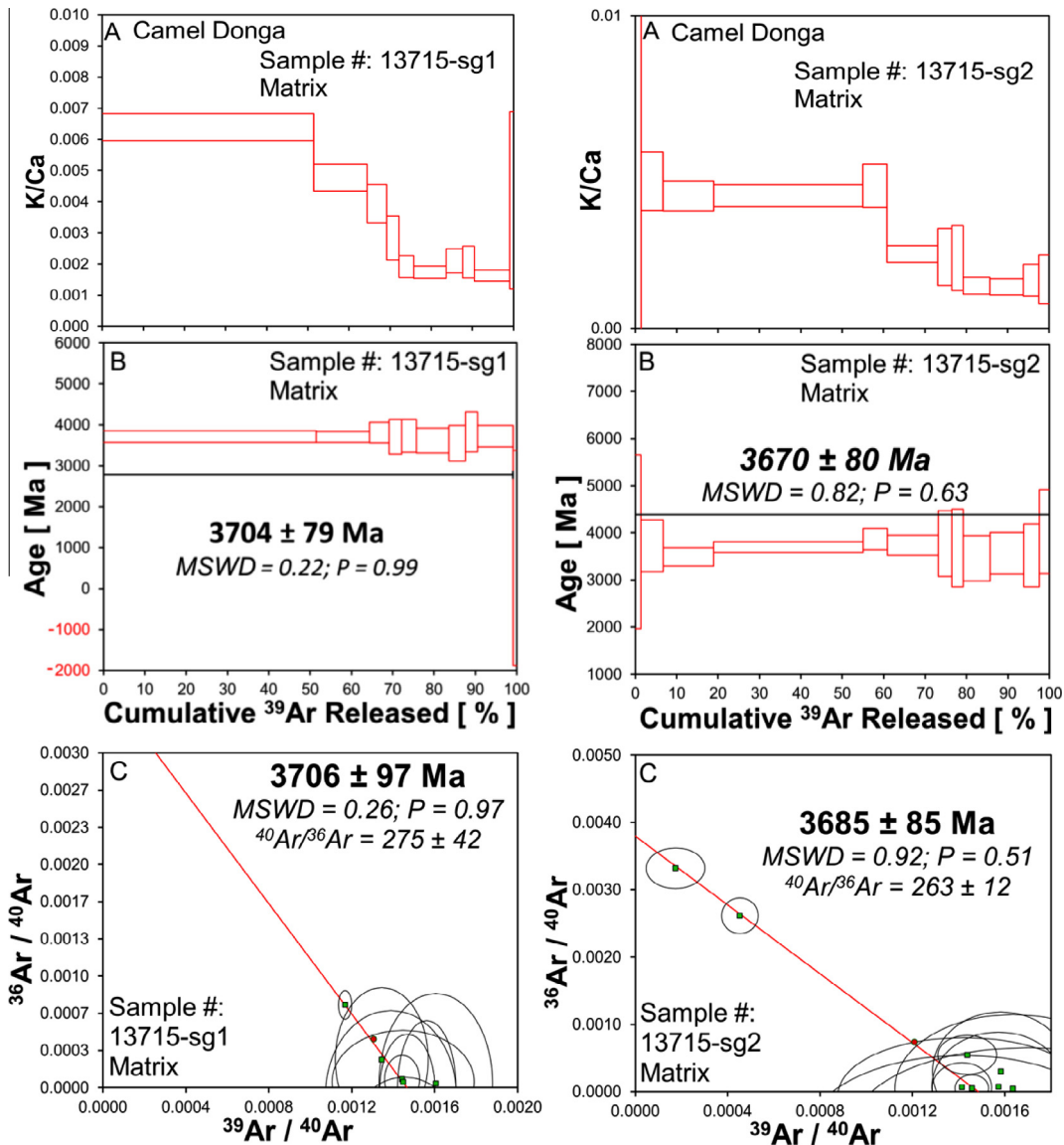


Fig. 2. Ar release spectra for Camel Donga. (A) K/Ca plot; (B) plateau age; and (C) inverse isochron. These plots of single grains of matrix show a weighted plateau age of 3693 ± 51 Ma recording a major impact event. In this and the following two figures (Figs. 3 and 4) plateau lines are represented by a solid black line and indicate those steps included in the age calculation, however the position on the y-axis does not represent this age.

4.1. Camel Donga (sample No. WAM13715)

13715-sg1 yielded a good plateau age of 3704 ± 79 Ma ($\text{MSWD} = 0.22$; $P = 0.99$) including 99% of ^{39}Ar (Fig. 2). The K/Ca (derived from $^{39}\text{Ar}_K/^{37}\text{Ar}_{\text{Ca}}$) plot shows a normal degassing profile where K-rich phases degas at relatively low temperatures and Ca-rich phases degas mostly at high temperatures. The inverse isochron plot shows that a significant amount of trapped Ar (probably due to atmospheric contamination; $^{40}\text{Ar}/^{36}\text{Ar} = 275 \pm 42$) was only released during the first of the incremental temperature extractions and all subsequent Ar was mostly radiogenic.

13715-sg2 also yielded a good plateau age of 3670 ± 80 Ma ($\text{MSWD} = 0.81$; $P = 0.63$) indistinguishable

from 13715-sg1, and including 100% of ^{39}Ar released (Fig. 2). The K/Ca plot is similar to that of 13715-sg1; initially high then gradually reducing and the inverse isochron plot shows that a significant amount of trapped Ar (probably due to atmospheric contamination; $^{40}\text{Ar}/^{36}\text{Ar} = 263 \pm 12$) was released during the first two of the incremental temperature extractions but with all subsequent Ar being mostly radiogenic.

The plateau ages for 13715-sg1 and -sg2 are within error and are combined into a weighted mean age of 3693 ± 51 Ma ($\text{MSWD} = 0.57$; $P = 0.93$).

Only one CRE age could be calculated for Camel Donga: 39.5 ± 4.5 Ma (13715-sg1; $\text{MSWD} = 0.54$; $P = 0.81$). The P -value of 13715-sg2 is 0.000; hence indicating that

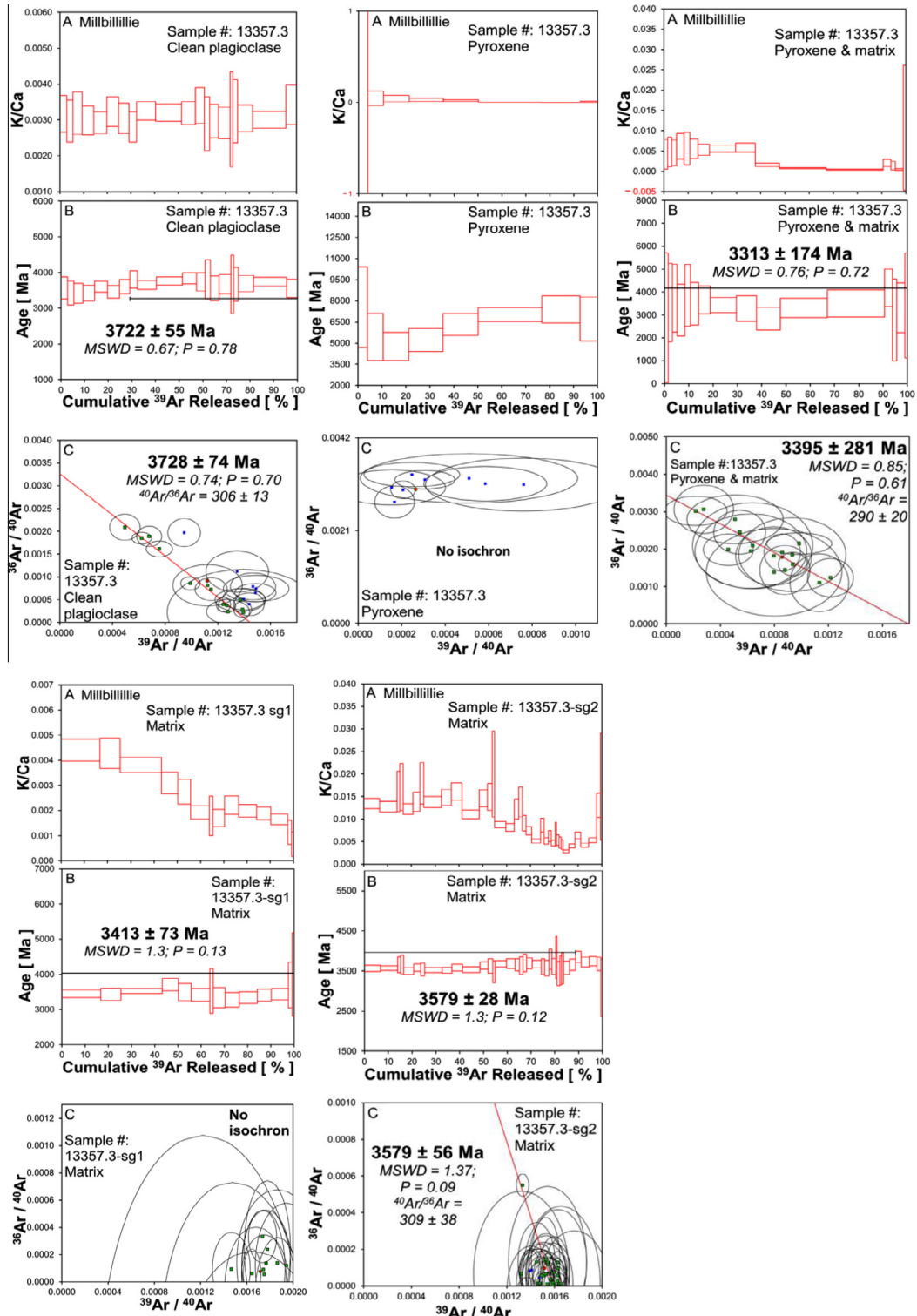


Fig. 3. Ar release spectra for Millbillillie. (A) K/Ca plot; (B) plateau age; and (C) inverse isochron. Three separate plateau ages are recorded by these plots: (1) plagioclase records a major impact event at 3722 ± 55 Ma; (2) matrix records a significant-sized impact at 3579 ± 28 Ma; and (3) pyroxene and matrix records a minor impact at 3313 ± 174 Ma.

its exposure age has been completely perturbed. 13715-sg1 has a robust P -value but it should be noted that virtually no spread is observed along the cosmochron making this exposure age suspect.

4.2. Millbillillie (sample No. WAM13357.3)

The aliquot of clean plagioclase (13357.3-plg clean; 10 grains) yielded a good plateau age of 3722 ± 55 Ma

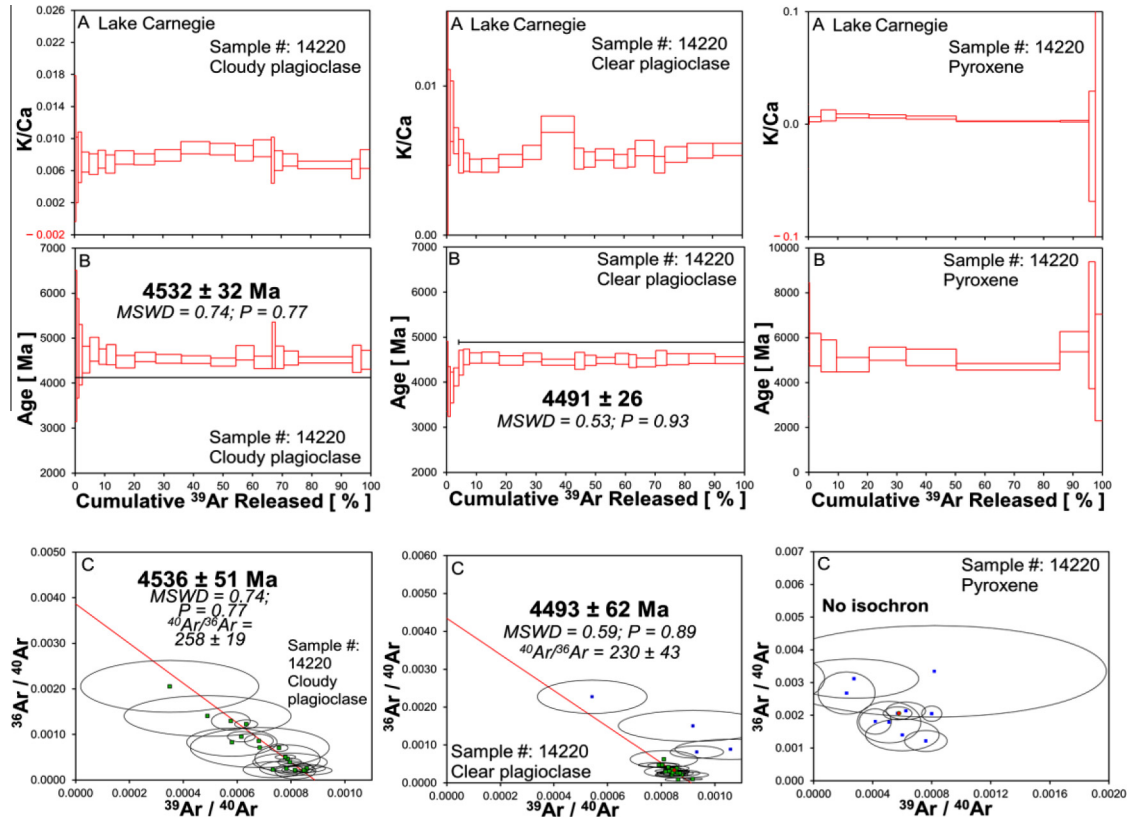


Fig. 4. Ar release spectra for Lake Carnegie. (A) K/Ca plot; (B) plateau age; and (C) inverse isochron. Plagioclase records a mega-impact event with a weighted plateau age of 4507 ± 20 Ma.

(MSWD = 0.67; $P = 0.78$) from 71% of ^{39}Ar released (Fig. 3), with the first part of the age spectrum showing signs of ^{40}Ar diffusive loss. The K/Ca plot shows a flat profile. The inverse isochron plot shows that a significant amount of trapped Ar, due to atmospheric contamination ($^{40}\text{Ar}/^{36}\text{Ar} = 306 \pm 14$), was released during the first seven steps of the incremental extractions, subsequently most of the ^{40}Ar released was radiogenic.

The pyroxene aliquot (13357.3-pyx; 12 grains) did not return a plateau age (Fig. 3). The K/Ca plot profile is flat. The inverse isochron plot shows that only trapped Ar was released over all temperature extractions so no inverse isochron could be calculated.

The sample consisting mostly of pyroxene (13357.3-pyx + matrix; 8 grains) but which included some with pyroxene with a matrix component yielded a well-defined, albeit imprecise, plateau age of 3313 ± 174 Ma (MSWD = 0.76; $P = 0.72$) calculated from 100% of ^{39}Ar (Fig. 3). The K/Ca plot shows two flat zones with K-rich phases degassing at lower temperatures and Ca-rich phases degassing at higher temperatures. The inverse isochron is well-defined with a spread of trapped and radiogenic argon ($^{40}\text{Ar}/^{36}\text{Ar}$ intercept = 285 ± 42).

A single grain (13357.3-sg1) of matrix yielded a plateau age of 3413 ± 73 Ma (MSWD = 1.3; $P = 0.13$) from 100% of ^{39}Ar (Fig. 3). The K/Ca (derived from $^{39}\text{Ar}_K/^{37}\text{Ar}_{\text{Ca}}$) plot shows K-rich phases degassing at lower temperatures grading into degassing of Ca-rich phases at higher temper-

atures. No inverse isochron age could be calculated due to the low spread along the isochron.

The second single grain (13357.3-sg2) of matrix yielded a plateau age of 3579 ± 28 Ma (MSWD = 1.3; $P = 0.12$) calculated from 89% ^{39}Ar (Fig. 3) and measured over higher resolution than 13357.3-sg1, and thus is thought to provide a more accurate picture of the impact history of Millbillillie. The K/Ca plot is curved with a gradual decrease from K-rich phases degassing at lower temperatures to Ca-rich phases degassing at higher temperatures. The inverse isochron plot shows a strong cluster indicating that radiogenic argon is dominant and the $^{40}\text{Ar}/^{36}\text{Ar}$ intercept = 310 ± 38 .

The CRE ages were: (1) clean plagioclase (13357.3-plg clean): 17.7 ± 1.3 Ma (MSWD = 0.26; $P = 0.99$), the P -value for this CRE age is robust with good spread along the cosmochron; (2) pyroxene (13357.3-pyx): no cosmic ray exposure age was obtained for this sample; (3) pyroxene and matrix (13357.3-pyx + matrix): this sample did not yield any concordant age (MSWD = 2.4; $P = 0.003$); (4) single grain of matrix (13357.3-sg1; Fig. 3) yields an imprecise CRE age of 34.8 ± 22.4 Ma (MSWD = 1.4; $P = 0.15$) which cannot be used due to the large uncertainty; (5) single grain of matrix (13357.3-sg2; Fig. 3): 16.9 ± 1.5 Ma (MSWD = 0.78; $P = 0.79$), this P -value is robust with a good spread along the cosmochron. A weighted mean exposure age for Millbillillie is 17.8 ± 0.9 Ma based on the two aliquots with a P -value ≥ 0.05 and concordant CRE ages.

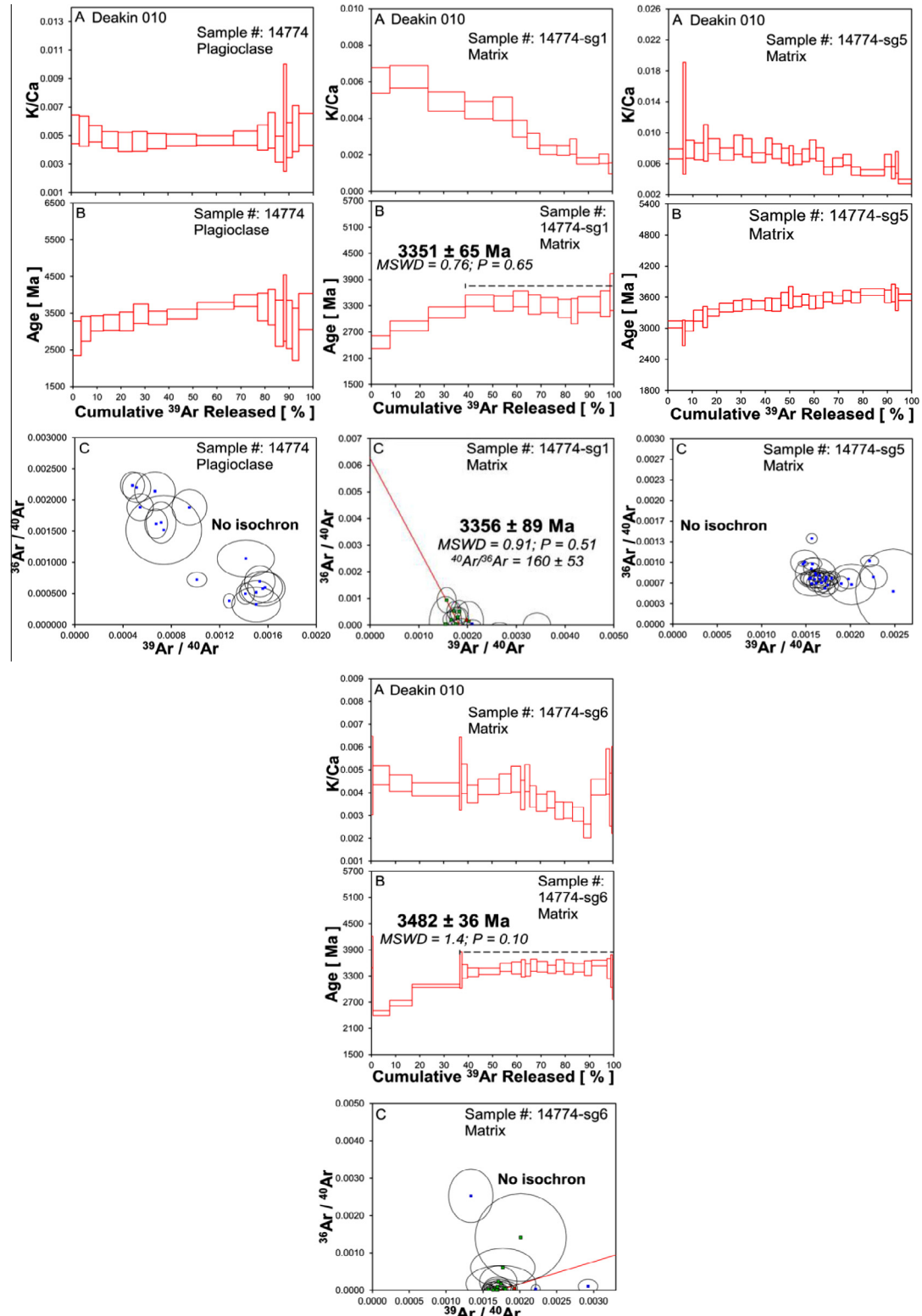


Fig. 5. Ar release spectra for Deakin 010. (A) K/Ca plot; (B) plateau age; and (C) inverse isochron. These spectra show that a restricted portion (i.e., $\leq 60\%$) of an age spectra cannot be used to derive an impact age and in most cases, yields only an intermediate meaningless age. In both this figure and Fig. 6 the trend of age spectra that did not achieve a plateau are shown by a dashed black line, however the position on the y-axis does not represent the age of the spectra.

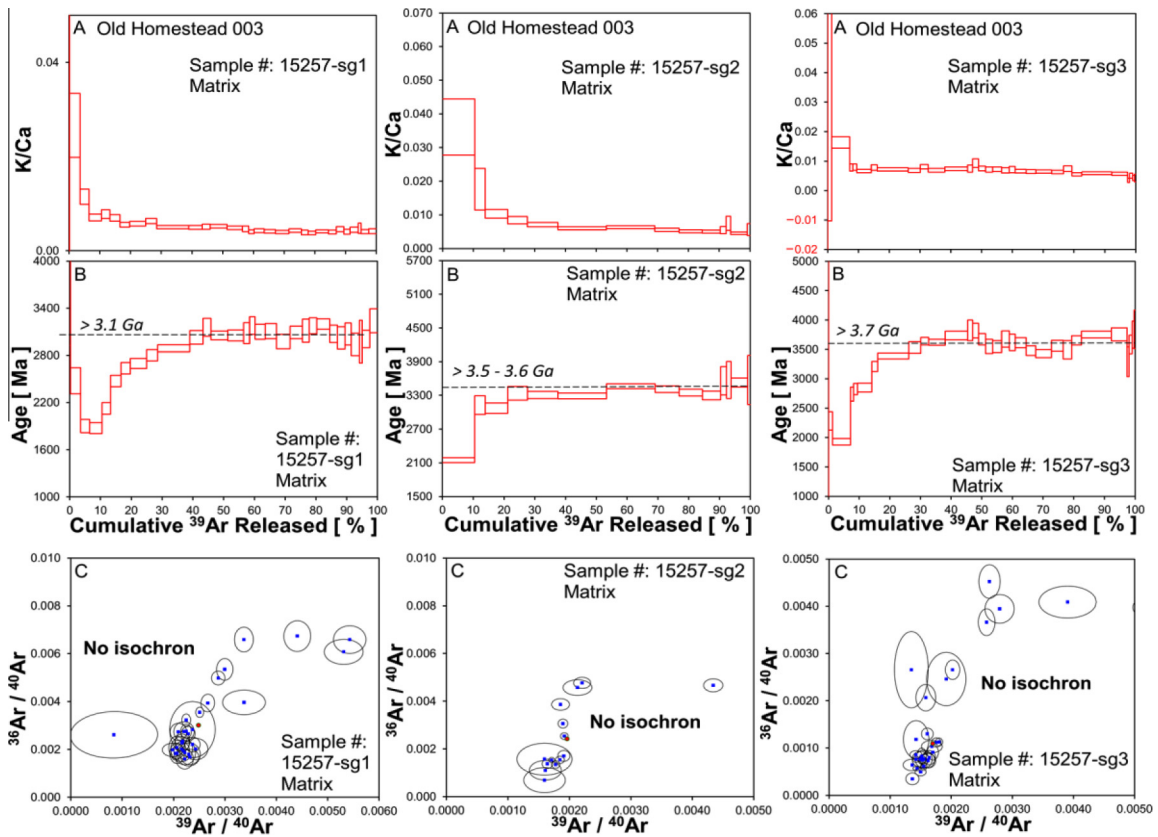


Fig. 6. Ar release spectra for Old Homestead 003. (A) K/Ca plot; (B) plateau age; and (C) inverse isochron. Three aliquots yielded ${}^{40}\text{Ar}^*$ diffusion loss profiles which provide only qualitative information of the major impacts that formed these melt rocks. An age of ~ 2 Ga age is common to all three aliquots, suggesting that the initial regolith material that is included in Old Homestead 003 was already assembled at this time.

4.3. Lake Carnegie (sample No. WAM14220)

The aliquot of cloudy plagioclase (14220-plg cloudy_1; 7 grains), gave a plateau age of 4532 ± 32 Ma (MSWD = 0.74; $P = 0.77$) calculated from 100% ${}^{39}\text{Ar}$ (Fig. 4), from a flat age spectra plot. The K/Ca plot was slightly curved although essentially flat. The inverse isochron yielded a trapped ${}^{40}\text{Ar}/{}^{36}\text{Ar}$ value of 259 ± 19 but most steps cluster near the radiogenic intercept.

The aliquot of clear plagioclase (14220-plg clear_2; 7 grains), gave a plateau age of 4491 ± 26 Ma (MSWD = 0.53; $P = 0.93$) calculated from 96% ${}^{39}\text{Ar}$ (Fig. 4), with the first four steps showing a diffusion profile over $\sim 4\%$ of the age spectrum. Trapped Ar due to atmospheric contamination (${}^{40}\text{Ar}/{}^{36}\text{Ar} = 238 \pm 108$) was only released over the first four incremental extractions. The K/Ca plot generally shows K-rich phases degassing at lower temperatures and then a fairly flat plot of Ca-rich phases degassing at higher temperatures; a brief spike represents a more K-rich phase degassing after about a 30% ${}^{39}\text{Ar}$ release. The inverse isochron plot shows a tight cluster of radiogenic Ar.

The pyroxene aliquot (14220-pyx; 15 grains) did not return a plateau age (Fig. 4) but seemingly suggests a relatively old (~ 4.5 Ga) age as well. The K/Ca plot is flat and shows K-rich phases only degassing at low-temperature

with no degassing of Ca-rich phases. The inverse isochron plot shows that only trapped Ar from atmospheric contamination was released over all temperature extractions.

A combined weighted mean of the two statistically indistinguishable plateau ages for the cloudy and clear plagioclase aliquots of Lake Carnegie gave an age of 4507 ± 20 Ma (MSWD = 0.81; $P = 0.79$).

The CRE ages were: (1) cloudy plagioclase (14220-plg cloudy_1): no cosmic ray exposure age was obtained for this sample (MSWD = 2.6; $P = 0.000$), the low P -value for this CRE age indicates that its exposure age has been completely perturbed although there is a good spread along the cosmochron; (2) clear plagioclase (14220-plg clear_2; Fig. 7): 6.2 ± 0.9 Ma (MSWD = 0.45; $P = 0.97$), this P -value is very robust and there is a good spread along the cosmochron; (3) pyroxene (14220-pyx): 6.6 ± 2.9 Ma (MSWD = 0.87; $P = 0.55$), this P -value is robust and the spread along the cosmochron is good. A weighted mean exposure age for the Lake Carnegie meteorite is 6.1 ± 0.9 Ma.

4.4. Deakin 010 (sample No. WAM14774)

For the Deakin 010 eucrite, we analysed plagioclase grains and several aliquots of single-grain matrix. The plagioclase aliquot (14774-plg_1; 10 grains) did not return a

Table 3
Calculated Cosmic Ray Exposure ages.

Sample name	Sample # prefix: WAM	Exposure age (Ma)	MSWD	P (>0.05)	Slope (2σ)	Weighted mean age for meteorite	MSWD	P (>0.05)
Camel Donga	13715-sg1	40 ± 5	0.54	0.81	0.0229 ± 0.0026			
Camel Donga	13715-sg2	No age	3.4	0.000	0.0204 ± 0.0013			
Camel Donga	13715 combo	No age	2.2	0.002	0.02055 ± 0.00079			
Millbillillie	13357.3-plg clean	18 ± 1	0.26	0.992	0.00905 ± 0.00067	17.8 ± 0.9	1.6	0.2
Millbillillie	13357.3-pyx	No age	—	—	—			
Millbillillie	13357.3-pyx + GM	No age	2.4	0.003	0.01039 ± 0.00079			
Millbillillie	13357.3-sg1	35 ± 22	1.4	0.15	0.0202 ± 0.013			
Millbillillie	13357.3-sg2	17 ± 2	0.78	0.79	0.00978 ± 0.00086			
Lake Carnegie	14220-plg cloudy_1	No age	2.6	0.000	0.00294 ± 0.00070	6.1 ± 0.9	0.4	0.53
Lake Carnegie	14220-plg clear_2	6 ± 1	0.45	0.97	0.00315 ± 0.00048			
Lake Carnegie	14220-plg combo	No age	1.6	0.017	0.00290 ± 0.00027			
Lake Carnegie	14220-pyx	7 ± 3	0.87	0.55	0.00338 ± 0.0015			
Deakin 010	14774-plg_1	15 ± 1	0.94	0.52	0.00766 ± 0.00065	Discordant ages between plagioclase and matrix		
Deakin 010	14774-sg1	9 ± 5	0.45	0.89	0.0053 ± 0.0028			
Deakin 010	14774-sg5	No age	—	—	1.00E-30 ± 4.7E-02			
Deakin 010	14774-sg6	No age	3.0	0.000	0.0059 ± 0.0035			
Old Homestead 003	15257-sg1	No age	—	—	—			
Old Homestead 003	15257-sg2	11 ± 9	0.0105	1.000	0.0054 ± 0.0045	Not enough spread along the cosmochron		
Old Homestead 003	15257-sg3	No age	2.1	0.001	0.00591 ± 0.00053			

Bold age indicates proposed CRE age for a given meteorite.

plateau age; the spectrum shows a slight rise at increasing temperature extractions and a final fall at high temperatures (Fig. 5), suggesting a minimum age of 3.7–3.8 Ga. The K/Ca plot is flat with slight rises at the lowest and highest temperature extractions. No inverse isochron age could be calculated.

The first single grain of matrix (14774-sg1) gave a mini-plateau age of 3351 ± 65 Ma (MSWD = 0.76; $P = 0.65$) calculated from 61% ^{39}Ar and the profile suggests diffusive ^{40}Ar was lost over the first 39% of the spectrum (Fig. 5). This gave a flat age spectrum plot after the first three extractions. The mini-plateau age of ~ 3.35 Ga probably represents the minimum age of an impact event. The K/Ca plot is a slope that is initially high then has a stable decrease that plateaus out towards the end. The inverse isochron shows no significant trapped argon, all argon being radiogenic. The samples released trapped Ar from atmospheric contamination ($^{40}\text{Ar}/^{36}\text{Ar} = 160 \pm 54$) only over the first three extractions; the remainder of the gas released was radiogenic.

14774-sg5 (matrix) did not return an age plateau (Fig. 5), but suggests a minimum age of ≥ 3.66 Ga. The age plot rises slowly to a gentle curve then slightly plateaus out before dropping over the last 10%. The K/Ca plot is generally flat, decreasing slightly over the last 35%. The inverse isochron plot shows data convergence towards the radiogenic axis.

14774-sg6 (matrix) gave a mini-plateau age of 3482 ± 36 Ma (MSWD = 1.4; $P = 0.1$) from 63% ^{39}Ar (Fig. 5) with an age spectra following a classical diffusion profile. The K/Ca plot is initially flat with an increase in

Ca-rich phases degassing between ~ 68 –90% ^{39}Ar released. No inverse isochron age could be calculated.

The CRE ages were: (1) plagioclase, 14774-plg_1: 15.0 ± 1.3 Ma (MSWD = 0.94; $P = 0.52$) with a good spread along the cosmochron; (2) matrix, 14774-sg1: 9.1 ± 4.8 Ma (MSWD = 0.45; $P = 0.89$) with a fair spread along the cosmochron; (3) matrix, 14774-sg5: no cosmic ray exposure age was obtained for this sample; (4) matrix, 14774-sg6 did not yield any concordant age. The plagioclase and matrix yielded different CRE ages; one explanation for this is the possibility that some of the plagioclase originally resided in material closer to the asteroid/meteoroid surface and was thus exposed to cosmic rays for a longer period than the comminuted matrix and that impact related mixing occurred significantly later in the history of the sample. Irradiation tracks are not visible in either plagioclase or pyroxene in this monomict achondrite suggesting that pre-compaction exposure did not take place.

4.5. Old Homestead 003 (sample No. WAM15257)

The first single grain, 15257-sg1, (matrix and melt) for this meteorite did not return a plateau age (Fig. 6). The spectra show a curved increase at increasing temperature extractions, this is characteristic of a diffusion profile converging toward a strict minimum age of >3.1 Ga, after an initial drop from the first to fourth extraction steps. The K/Ca plot is flat after an initial degassing of K-rich phases. No inverse isochron age could be calculated.

15257-sg2 (matrix and melt) did not return a plateau age (Fig. 6) and exhibits a typical diffusion profile converging

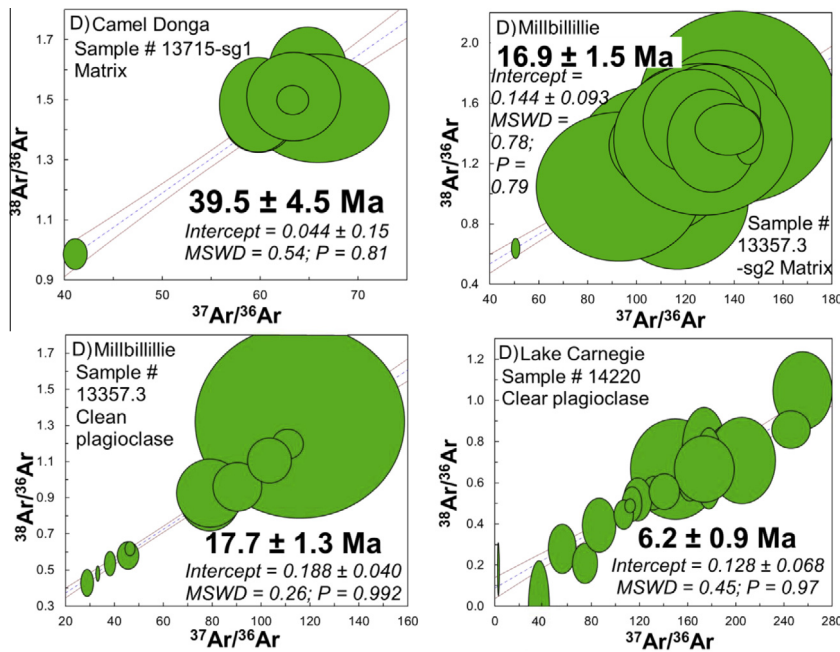


Fig. 7. Cosmic Ray Exposure age plots. Examples of four CRE age plots for: (1) Camel Donga; (2) Millbillillie – 2 examples; and (3) Lake Carnegie.

toward a minimum age of >3.5 – 3.6 Ga. The K/Ca plot declines over the first four low-temperature extractions then plateaus out. No inverse isochron age could be calculated.

The third grain, 15257-sg3, (matrix and melt) also did not return a plateau age (Fig. 6) but shows a diffusion profile that defines a minimum age of >3.7 Ga at high-temperature. The K/Ca plot is initially high then plateaus out. No inverse isochron age could be calculated.

The CRE ages were: (1) 15257-sg1, matrix and melt: no cosmic ray exposure age was obtained for this sample; (2) 15257-sg2, matrix and melt: 11 ± 9 Ma (MSWD = 0.0105; P = 1.000), this P-value is robust but with almost no spread along the cosmochron; (3) 15257-sg3, matrix and melt: no cosmic ray exposure age was obtained for this sample, the data indicate that the exposure age has been completely perturbed. Consequently no CRE age could be obtained for this sample.

5. DISCUSSION

5.1. Significance of the $^{40}\text{Ar}/^{39}\text{Ar}$ and CRE ages

5.1.1. Camel Donga (sample No. WAM13715): Record of a large impact at ~ 3.7 Ga

The two ages obtained for this eucrite (3704 ± 79 Ma and 3670 ± 80 Ma) represent significant thermal degassing best interpreted as reflecting a single major impact on Camel Donga's parent body with a weighted mean age of 3693 ± 51 Ma. The two aliquots yielded 99% and 100% plateau age spectra respectively, and they do not show any sign of subsequent disturbance likely to be associated with secondary minor impacts. The impact that ejected Camel Donga from its parent body, at a minimum age of ~ 40 Ma, did

not affect the K/Ar system within the matrix. This sample yielded one of the least disturbed K/Ar systematics recorded by any brecciated eucrite sample so far (cf. discussion below).

5.1.2. Millbillillie (sample No. WAM13357.3): Three impact events recorded in a single sample

The $^{40}\text{Ar}/^{39}\text{Ar}$ technique has yielded three plateau (that include 70% of ^{39}Ar released or more) ages from separate phases of a single meteorite: Millbillillie, by careful separation of plagioclase, matrix, and pyroxene. This has resulted in the definition of three thermal events thus confirming the ability of the K/Ar system to record different magnitudes of impact in different phases from a single sample (e.g., see discussion in Cassata et al., 2011). The preservation of different impact events in these phases is possible at very high-temperature (c.f. discussion below). Matrix is essentially a mixture of phases but with such small mineral components that it behaves as single average entity and gives intermediate diffusion characteristics between plagioclase and pyroxene rather than being a true physical mixture of the two separate phases.

In the study presented here, it is interpreted that the plagioclase (13357.3-plg clean; Fig. 3) represents the most retentive phase (at least as far as high-temperature flash-heating is concerned, cf. discussion by Cassata et al., 2010 and below) of the eucrite and has recorded a major impact event at 3722 ± 55 Ma. There are hints of a subsequent partial-reset in the first few steps of the plagioclase Ar spectrum that indicate a minimum reset age of ~ 3.5 – 3.6 Ga, but the well-defined plateau age suggests that these events did not substantially affect the K/Ar system which

has essentially preserved the age of the large impact. The second matrix sample (13357.3-sg2; Fig. 3) shows a plateau age of 3579 ± 28 Ma suggesting that the matrix has been completely reopened at this time, most probably by a significant-sized impact, although this impact was not large enough (i.e., did not provide enough heat) to significantly reset the K/Ar clock of the plagioclase. Different plateau ages from the plagioclase and the matrix along with convergence of the apparent ages of the lowest temperature steps of the plagioclase at ~ 3.6 Ga argue in favour of two impacts with two different ages being recorded in the same sample.

The K/Ca ratio of 0.00065 ± 0.00032 (2σ) of sample (13357.3-pyx + matrix; Fig. 3) suggests that it is mostly composed of pyroxene although minor matrix is also present. This sample yielded a plateau age at 3313 ± 174 Ma (the larger error is due to the low K₂O contained in the pyroxene) that suggests that pyroxene has been reset at this time. This would mean that this impact event is younger than the ones recorded by the plagioclase (~ 3.7 Ga) and second matrix sample (13357.3-sg2; ~ 3.6 Ga) but has not affected these two phases.

The age difference between matrix or plagioclase, and pyroxene is not surprising as Cassata et al. (2011) showed recently that Ar diffusion in pyroxenes can be extremely rapid for high-temperature events that are too brief to affect other phases such as plagioclase (i.e., due to the kinetic crossover of the D_0/r^2 values of pyroxene and plagioclase at high-temperature). Their findings suggest that pyroxene is the most likely mineral phase to record brief, high-temperature shock heating events generally associated with small, localised impacts. Therefore, we suggest that, although relatively imprecise, the age recorded by the pyroxene phase reflects a minor impact at ~ 3.3 Ga. More surprising is the resolvable age difference between 13357.3-sg1 (~ 3.41 Ga; Section 4.2) and 13357.3-sg2 (~ 3.58 Ga) as both single-grain aliquots consist of what seems to be pure matrix, but see discussion below.

In summary, Millbillillie displays internally consistent evidences for a major impact at ~ 3.72 Ga, a moderate impact at ~ 3.58 Ga, and a later small impact at ~ 3.3 Ga which did not reset the ages of the plagioclase or matrix. That all three ages are related to impacts rather than recording magmatic crystallisation and two subsequent impacts is based on the absence of any data recording magmatic activity after ~ 4.4 Ga (Tera et al., 1997), otherwise we would be unable to rule out magmatic crystallisation at ~ 3.72 Ga.

5.1.3. Evidence of mixed phases and mixed ages

Although 13357.3-sg1 (matrix; Fig. 3) gave a plateau age of 3413 ± 73 Ma (albeit with a borderline P -value of 0.13), a closer look at the age spectrum suggests that a level of perturbation, masked by the low resolution obtained on the age of each individual step, seems to exist. The shape of the age spectrum and K/Ca plot suggest that the low-temperature part of the spectrum reflects a dominant degassing of the matrix (mean age of ~ 3.5 Ga; relatively high K/Ca ratio) whereas the latter part of the spectrum is dominated by the younger pyroxene phase (mean age of

~ 3.4 Ga; relatively low K/Ca compared to matrix and similar to 13357.3-pyx). Therefore, we interpret this age spectrum as reflecting a mixture of ages obtained from different mineral components (by opposition to a pure single “matrix” component). Consequently, we suggest that the apparent age given by this aliquot does not reflect a true age of an impact event, but a mixed age between pyroxene and matrix phases.

5.1.4. Lake Carnegie (sample No. WAM14220): Impact or cooling at ~ 4.51 Ga?

The two plagioclase aliquots yielded two indistinguishable, very well-defined plateau ages of 4532 ± 32 Ma and 4491 ± 26 Ma for the Lake Carnegie unbreciated cumulate eucrite. The combined weighted mean age of 4507 ± 20 Ma could either represent a crystallisation age, a metamorphic age due to burial, or an impact age. Whatever the cause, this thermal event must have occurred soon after asteroidal differentiation, crystallisation and subsequent metamorphism. The oldest calcium aluminium inclusions (CAIs) in meteorites, have been dated at 4568 ± 2 Ma (Wadhwa et al., 2006) within error of a ^{207}Pb – ^{206}Pb internal isochron absolute crystallisation age of 4566.5 ± 0.2 Ma from the basaltic meteorite Asuka 881394, showing that the parent body for this meteorite was fully accreted within ~ 0.5 Ma of the formation of the Solar System (Wadhwa et al., 2009). Lugmair and Shukolyukov (1998) have shown from ^{53}Mn – ^{53}Cr systematics that the last global fractionation of Mn/Cr in the HED parent body mantle, occurred 4564.8 ± 0.9 Ma ago and this is very close to the best estimate for the crystallisation age of the Sahara 99555 angrite from whole rock ^{207}Pb / ^{206}Pb vs. ^{204}Pb / ^{206}Pb isochron established by Amelin (2008); also supporting very early accretion and differentiation of basaltic bodies in the early Solar System. Kleine et al. (2002) note that their revised date for mantle – crust differentiation on Vesta, 4.2 ± 1.3 Ma after the beginning of the Solar System, is in agreement with ages obtained by the ^{53}Mn – ^{53}Cr (Lugmair and Shukolyukov, 1998), ^{60}Fe – ^{60}Ni (Shukolyukov and Lugmair, 1993) and ^{26}Al – ^{26}Mg (Srinivasan et al., 1999) chronometers. Nevertheless, the HED parent body was probably still experiencing high temperatures up to 100 Ma after that (Ghosh and McSween, 1998), as seen in the equilibration and annealing textures of pyroxene in many cumulate eucrites including Lake Carnegie. Such a duration largely overlaps with the weighted mean age obtained in this study which, in principle, would suggest that the ^{40}Ar / ^{39}Ar age recorded by Lake Carnegie reflects cooling below the closing temperature of plagioclase of ca. 250–300 °C (Cassata et al., 2009), however, an early mega-impact cannot be discounted. Here, two scenarios are proposed based on ^{40}Ar / ^{39}Ar data alone.

1. The ~ 4.51 Ga age reflects a cooling age of the external layers of the asteroid. This hypothesis is supported by the absence of shock features and the undisturbed retention of metamorphic neoblasts and symplectitic textures, formed as the last products of a cooling magma. If the coarse-grained and annealed Lake Carnegie equilibrated at a similar or slightly shallower depth, c. 8 km, to the

- similarly textured cumulate eucrite Moore County (Miyamoto and Takeda, 1994); then a *significant impact* would be required to excavate it. In this scenario, the unbreciated eucrites would be located too deep in the asteroid to be affected by the shock wave created by the giant impact. Such an impact could have therefore happened at anytime in the history of the asteroid as no particular time constraint is required by this scenario, since the mega-impact had no effect on the K/Ar age of the plagioclase. In any case, the relatively small target size and perhaps accompanying insignificant gravity pool of the ejected chunk (secondary asteroid) ensured that it was not subject to the continuing impact history experienced by its much larger parent asteroid (as evidenced by the group of brecciated eucrites and howardites).
2. The ~4.51 Ga age recorded the mega-impact that ejected a major chunk of the asteroid and the Lake Carnegie plagioclase K/Ar system has not been reset by subsequent impact events, despite the fact that relatively small impact events can cause minor $^{40}\text{Ar}^*$ diffusion from the low-retentivity sites (not seen in the Lake Carnegie age spectra; Fig. 4). The absence of shock features reflects the fact that Lake Carnegie was buried deep in the asteroid, far from the impact location, but could have still been opened by the impact-related heat wave or perhaps, rather paradoxically, rapidly cooled down if it was still hot (above K/Ar plagioclase closure temperature) at the depth at which Lake Carnegie was located when the impact related excavation occurred (see discussion by Bogard, 2011). In this scenario, the impact that ejected the chunk of asteroid (including Lake Carnegie) from its parent body happened at ~4.51 Ga and as suggested in the first scenario, the small size and low gravity field of the secondary asteroid prevented it from being pummelled by subsequent major impacts.

One way of determining which of these two scenarios is most likely is to compare a series of precise and accurate $^{40}\text{Ar}/^{39}\text{Ar}$ analyses to test whether all ~4.5 Ga unbreciated eucrites have identical $^{40}\text{Ar}/^{39}\text{Ar}$ ages or not. In theory, a range of well-defined *plateau* ages over a few tens of Ma from different unbreciated eucrites would argue for different cooling ages, probably due to their origins at various depths; this scenario would be even more favoured if the ages correlated with petrographic depth indicators. On the other hand, a series of samples all yielding an identical age would suggest that such an age reflects a large impact event, especially if the same age is obtained for a series of unbreciated eucrites with different depth indicators. Note that in the case of rapid cooling, the relatively large uncertainty associated with $^{40}\text{Ar}/^{39}\text{Ar}$ ages might mask subtle age differences and therefore, an apparent age synchronicity between all unbreciated eucrites would not completely rule out the cooling age scenario. We compare our new age with published ~4.5 Ga ages below.

Again, in both scenarios, it is likely that the small size of the resulting secondary asteroids prevented them from

being impacted by large asteroids which left the ~4.5 Ga K/Ar ages undisturbed.

5.1.5. Deakin 010 (sample No. WAM14774): The problem of apparent ages

The apparent mini-plateau and minimum ages of 3351 ± 65 Ma, 3482 ± 36 Ma and ≥ 3.7 Ga, obtained from this meteorite are from 3 single grains of matrix (a mix of comminuted pyroxene, plagioclase and amorphous silica phase) derived from the same sample. At this sample scale (<1 mm in diameter), it is expected that any mineral or melt phase would record a single impact event, unless components from different origins have been brought together later in their respective history, as is the case for howardite meteorites. However, this brecciated, monomict basaltic rock is unlikely to contain such unrelated clasts and this would therefore suggest that the same history should be observed in all parts of the sample, which is clearly not the case.

Regardless of the significance of the apparent $^{40}\text{Ar}/^{39}\text{Ar}$ ages recorded by Deakin 010, these data suggest that during impacts, the energy is not equally distributed at the *sample scale*, with aliquots 14774-sg1 (~3.35 Ga) being more degassed than 14774-sg6 (~3.48 Ga) and especially 14774-sg5 (≥ 3.7 Ga). With that in mind, the significance of these dates is open to interpretation. Do they reflect true thermal shock events caused by several distinct impacts or are they unresolvable ‘apparent’ ages? Whereas 14774-sg5 only converges towards a minimum age of ≥ 3.7 Ga, the other two samples developed mini-plateau over more than 60% of ^{39}Ar released, following a clear ^{40}Ar diffusion loss pattern (Fig. 5). Experiments have shown that such diffusion profiles, unless they include a minimum of 70% of ^{39}Ar released, will generally converge towards a minimum age at high-temperature where the apparent age given by a mini-plateau can be offset by several tens of Ma compared to the true age of the initial event being tentatively measured (e.g., see examples in Cassata et al., 2009). Therefore, at face value the mini-plateau ages of ~3.4 and ~3.5 Ga would reflect subsequent partial-reset of an initial impact event that occurred prior to ~3.7 Ga.

The age of the subsequent impact that partially reset the K/Ar system of 14774-sg1 and 14774-sg6 is younger than or equal to ≤ 2.4 Ga, as given by the youngest low-temperature steps of both 14774-sg1 and 14774-sg6. However, some atmospheric Ar may be present in the first steps raising the possibility that the low-T $^{40}\text{Ar}^*$ loss is recent grain surface weathering and not a <2.4 Ga impact. The fact that different aliquots of the same sample yielded various mini-plateau ages shows that a restricted portion (i.e., $\leq 60\%$) of an age spectra cannot be used to derive an impact age and in most cases, yields only an intermediate meaningless age. Only robust plateaus unambiguously record significant thermal events. Mini-plateaus can still reveal impact ages, if and only if, different aliquots give reproducible and concordant ages. As previously suggested by Jourdan et al. (2009) and Jourdan (2012), this study prompts us to recommend that only single grains of material be analysed (when possible) to avoid the effect of mixing of multiple grain aliquots with various Ar retention histories, even at the single bulk

sample level. Therefore, from this discussion it can be argued that whilst the data we present here fall within the age range proposed by Bogard and Garrison (2003) of 4.1–3.1 Ga, the true age range of major impacts may be more restricted. We also reiterate that Deakin 010 is an anomalous achondrite and as such $^{40}\text{Ar}/^{39}\text{Ar}$ ages obtained for this meteorite cannot help constrain the bombardment history of the HED parent body.

5.1.6. Old Homestead 003 (sample No. WAM15257)

This howardite, as regolith material, contains a range of impact material that has recorded various impact events, probably distributed over a significant portion of the surface of the HED parent body. Impact melt forms a component of the matrix and plagioclase has also been converted to maskelynite as part of the thermal impact process. The lack of plateau ages in this regolith material is attributed to the complex number of impact related thermal events experienced on the asteroid's surface, as confirmed by images of 4 Vesta from the NASA Dawn Mission probe (NASA, 2011).

The three aliquots of single grains comprised of matrix/melt material yielded $^{40}\text{Ar}^*$ (radiogenic argon – produced from the natural decay of ^{40}K) diffusion loss profiles which provide only qualitative information. Assuming that these grains record a single impact, this must be older than >3.7 Ga, however, due to the regolith nature of howardites, it is possible that these matrix/melt rock grains were formed during different impacts, whose ages cannot be constrained by these data except that they are older than 3.1, 3.6 and 3.7 Ga. All three aliquots showed low-temperature step ages that converge toward ~2 Ga, this suggests a minimum age for an impact event that affected the regolith of the parent body of Old Homestead 003. As the three apparent ages given by the low-temperature steps are similar, they might approach the true age of the thermal event that partially reset these grains (i.e., ~2 Ga). As a comparison, a high-resolution $^{40}\text{Ar}/^{39}\text{Ar}$ thermochronometry study of lunar regolith rocks by Shuster et al. (2010) found evidence for a systematic partial resetting of the K/Ar systems of several regolith samples estimated to have occurred at ~3.3 Ga. Similarly, this age estimate is based on converging low-temperature degassing step ages, which they conclude is related to a single impact event at this time (see discussion in Shuster et al. (2010)). In the case of Old Homestead 003, as a ~2 Ga age is common to all three aliquots, it is highly likely that the initial regolith material was already assembled at this time. It is also possible that the impact forming Old Homestead was responsible for the partial degassing of the samples.

Marchi et al. (2012) have suggested an age, calculated from crater counting using Dawn Mission¹ imaging, of ca. 1–2 Ga for both the Rheasilvia and Veneneia basins. This age range is not in agreement with the older ages of >3.1, >3.6 and >3.7 Ga recorded by Old Homestead 003, however the crater counting method of age dating may not tightly constrain the basin age due to secondary crater-

ing effects on calculations (McEwen and Bierhaus, 2006). Additionally, images from the Dawn Mission show that there have been significant landslides and slumping around crater rims causing crater erasure, and hence craters within the Veneneia and Rheasilvia basins may have been obscured.

5.2. Implications for early (~4.5 Ga) thermal events on the HED parent body

Evidence for the youngest basaltic volcanism on the HED parent body comes from coarse-grained, mesostasis-rich basaltic clasts in the polymict eucrite Y 75011, in which the pyroxenes have retained their original extensive Fe–Mg zoning (Takeda and Graham, 1991). The largest clast revealed Rb–Sr ages of 4600 ± 50 Ma and 4500 ± 50 Ma (depending on the ^{87}Rb decay constant used) and a Sm–Nd isochron age for clasts and matrix of 4550 ± 140 Ma (Nyquist et al., 1986). These ages are not tightly constrained, but they do include the more precise plateau age obtained here for Lake Carnegie cumulate eucrite (4507 ± 20 Ma). Cumulate eucrites have been shown to have younger ages of <4480 Ma as they cooled over a longer time span compared to basalts that cooled quickly at or very near the surface (see references in Carlson and Lugmair, 2000).

Our $^{40}\text{Ar}/^{39}\text{Ar}$ age for Lake Carnegie (4507 ± 20 Ma) records an event within $\sim 60 \pm 20$ Ma of the beginning of the differentiation of the HED parent body (Lugmair and Shukolyukov, 1998), and as outlined above, we suggest that this age might be associated with either a major impact event on the HED parent body or cooling below the K/Ar closure temperature of plagioclase following differentiation and crystallisation on the HED parent body. The coarse-grain size and post crystallisation, slow subsolidus equilibration and annealing textures of pyroxene in Lake Carnegie are shown in Fig. 1c.

The majority of $^{40}\text{Ar}/^{39}\text{Ar}$ data in the literature, although indicating a similar age of ~4.5 Ga (e.g., Bogard and Garrison, 2003 but see also discussion by Bogard, 2011), cannot be used to discriminate between the two scenarios proposed above as they unfortunately do not define the statistically valid ages that are required to test absolute synchronicity. Only a handful of results can be used, for example Yamaguchi et al. (2001) obtained $^{40}\text{Ar}/^{39}\text{Ar}$ plateau ages of 4490 ± 29 Ma and 4485 ± 28 Ma (recalculated using Renne et al., 2010 and including all sources of uncertainties) on two clasts of EET90020 (EET90020,26 and EET90020,22) as well as a concordant Sm/Nd age of 4510 ± 40 Ma. It is worth noting that a few Pb–Pb and Sm/Nd ages of unbreciated eucrites have been published, however as both systems are resistant to shock resetting, the age they record is most likely to be magmatic. Therefore, in order to test our single giant impact scenario, we will compare data obtained solely from an impact-sensitive isotopic chronometer: $^{40}\text{Ar}/^{39}\text{Ar}$. As such, the three $^{40}\text{Ar}/^{39}\text{Ar}$ ages (EET90020,26 and EET90020,22 and Lake Carnegie) are concordant (weighted mean age of 4497 ± 14 Ma; MSWD = 0.98; $P = 0.37$) within errors, suggesting that a major impact event might have occurred

¹ Dawn Mission article: <http://www.bbc.co.uk/news/science-environment-15286950>.

on the HED parent body at ~ 4.50 Ga, early in the history of formation of the Solar System. If true, this impact must have been very large as it released a series of unbrecciated eucrites without any evidence of impact, for instance shocked minerals and impact-related melt. Such a mega-impact would have released the Lake Carnegie meteoroid from the HED parent body, allowing it to escape further impact events that were experienced by the parent body. A similar scenario was proposed by Bogard and Garrison (2003) for unbrecciated eucrite $^{40}\text{Ar}/^{39}\text{Ar}$ ages clustering around ~ 4.48 Ga. However, it should be kept in mind that the relative errors of individual ages are still large and this apparent synchronicity must be tested by further experiments, preferably using the same experimental conditions and isotopic technique (e.g., plagioclase $^{40}\text{Ar}/^{39}\text{Ar}$ dating) to make sure that the exact same geological event is recorded. At this stage, future dating campaigns of unbrecciated eucrites are required before firm conclusions can be drawn.

5.3. Post 4.5 Ga impact history of the HED parent body

Filtering of published $^{40}\text{Ar}/^{39}\text{Ar}$ age data resulted in none of the post-4.5 Ga brecciated eucrites defining a statistically valid plateau age (i.e., including more than 70% ^{39}Ar released). Although this filtering threshold may appear harsh, it should be noted that the overwhelming majority of the published dates on brecciated HED meteorites are based on perturbed age spectra (e.g., Bogard and Garrison, 2003), upon which data interpretation is both uncertain and user-dependent. For example, in this study the results from Deakin 010 show a series of discordant (Fig. 5) mini-plateau ages recorded in several aliquots from a single matrix sample. More importantly, these mini-plateaus are *better defined* that the overwhelming majority of age spectra found in the literature and yet do not seem to produce any quantitative information about impact ages. Hence, for the purpose of this study, we choose to retain only well-defined plateau ages most likely to represent the true age of impacts.

Altogether, we obtained four new impact ages recorded by two meteorites and related to impacts of various sizes and strengths. Camel Donga and Millbillillie record a time span of large impacts from 3722 ± 55 Ma to 3579 ± 28 Ma as recorded by plagioclase and matrix aliquots (Figs. 2 and 3). Smaller impacts, recorded either by pyroxene or by low-temperature steps of melt rock and plagioclase suggest that minor impacts occurred down to at least 3313 ± 174 Ma. We note that Nyquist et al. (1997) obtained an age of 3460 ± 180 Ma on matrix for the monomict eucrite Y-791186, 87; within the age range recorded by Camel Donga and Millbillillie. Deakin 010 and Old Homestead 003 failed to give any plateau age and only provide qualitative information, similar to most of the published HED $^{40}\text{Ar}/^{39}\text{Ar}$ data.

In summary, plagioclase records a group of ages ranging between ~ 3.7 and 3.6 Ga, while the matrix records an age group between ~ 3.6 to 3.5 Ga. Finally, pyroxene and low-temperature steps record subsequent minor impact events from ~ 3.4 to 3.3 Ga, which were not of sufficient en-

ergy to reset the older thermal events recorded by plagioclase. This apparent reduction in significant impact events with time, albeit on a very small population, may reflect the disassembly of the asteroid belt as the Solar System matures; however, it is also possible that any pre-existing small impacts events have been reset. If this second scenario is correct then it might be expected that a higher degree of melting would have occurred in the significant impact event because the initial small impacts would pre-process the grains making them more susceptible to melting. As we do not see evidence for this in Millbillillie these data may well record a decrease in size of impacts with time, but more data are required to confirm this.

An obvious (and already known) implication of these results is that after the early mega-impact that ejected the unbrecciated eucrite clan, further impact events on the HED parent body occurred. However, the limited dataset derived from robust plateau ages only, suggests that a massive bombardment of large objects might have occurred over a more restricted time range (~ 3.8 – 3.5 Ga) than that previously suggested (i.e., ~ 4.1 – 3.4 Ga; e.g., Bogard and Garrison, 2003, or ~ 500 Ma: Bogard, 2011); more $^{40}\text{Ar}/^{39}\text{Ar}$ ages are required to further test this theory. In addition, it appears that most of the impacts that left well-defined ages occurred later than the age range of 4.1– 3.8 Ga associated with the Late Heavy Bombardment hypothesis (Gomes et al., 2005). These new ages are shown in Fig. 8, defining a restricted interval of impact events. It is also worth noting that a major impact of similar age has also been recorded on the parent body of anomalous eucrite Bunburra Rockhole (seven concordant $^{40}\text{Ar}/^{39}\text{Ar}$ plateau ages with a weighted mean of 3634 ± 18 Ma; Jourdan et al., 2011).

5.4. Major impacts of 4 Vesta

With the hypothesis that the HED meteorite clan belong to the asteroid 4 Vesta, we can now ask how the ages obtained here relate to the cratering observed on this asteroid by the NASA Dawn Mission studies (Marchi et al., 2012). Recent imagery show that a much older impact crater (“Veneneia”, ~ 350 – 400 km in diameter) partially underlies the ~ 500 km diameter southern hemisphere crater known as Rheasilvia (O’Brien et al., 2012; Schenk et al., 2012). It is possible that either of the impacts could have released the vestoid family of asteroids, although the ages of these craters are currently not tightly constrained, being based on crater counting and orbital projections. Note that crater counting on a small body such as 4 Vesta is difficult to fully calibrate without isotopic ages. For example, Marzari et al. (1996) suggested that the age of the vestoid family of asteroids is ~ 1 Ga based on orbital projection evidence. Typically, only in situ isotopic ages would allow the ages of these mega-impacts to be determined with confidence. However, the $^{40}\text{Ar}/^{39}\text{Ar}$ ages presented here have identified two significant impact events that completely reset the K/Ar systems (i.e., yielded well-defined plateau ages) in three eucrites: Lake Carnegie (4507 ± 20 Ma), Camel Donga (3693 ± 51 Ma) and Millbillillie (3722 ± 55 Ma), which represents the age of the largest impact, recorded by the

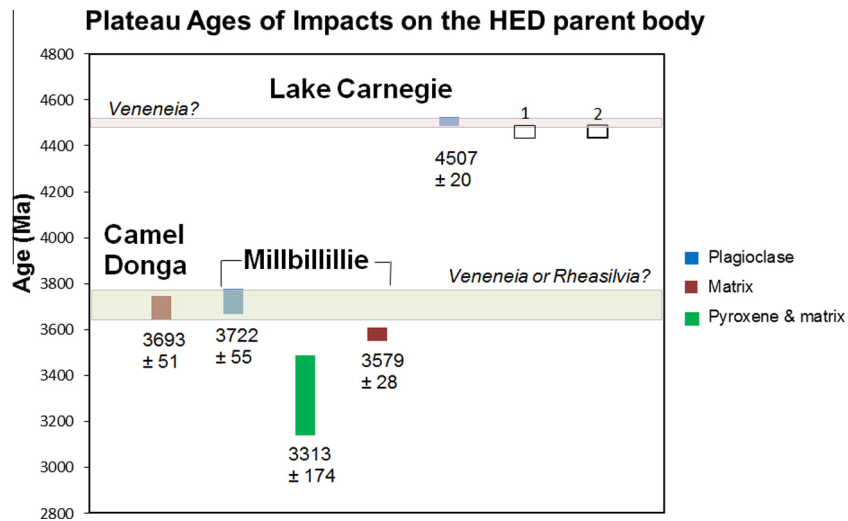


Fig. 8. Plateau ages summary plot from Camel Donga, Millbillillie and Lake Carnegie. A plot of well-defined plateau ages only, showing the restricted time range of impact events experienced by these meteorites; (1) whole-rock $^{40}\text{Ar}/^{39}\text{Ar}$ age for EET90020,26 (Yamaguchi et al., 2001); 2) whole-rock $^{40}\text{Ar}/^{39}\text{Ar}$ age for EET90020,22 (Yamaguchi et al., 2001).

plagioclase from this meteorite). The Lake Carnegie age could be interpreted to represent a mega-impact at 4.5 Ga that ejected a complete secondary parent body which included all the unbrecciated eucrite family; while the latter two ages are interpreted as indicating a giant impact at ~ 3.7 Ga on the HED parent body.

If the HEDs are indeed from 4 Vesta, then the two ages of the mega-impact events could be the two large impact basin forming events on 4 Vesta. Based on well-defined impact ages, we propose two scenarios:

Scenario (1): the Lake Carnegie age of ~ 4.51 Ga could represent the mega-impact that excavated the south polar Veneneia basin that underlies the younger Rheasilvia impact basin. This would require excavation of the Lake Carnegie material at that time, as its age has not been reset by further impacts due to the small size of the secondary asteroid; and (2) that impact age data suggest that, while the bombardment of large objects lasts from ~ 3.8 to ~ 3.5 Ga, there is a small concentration of well-defined ages around ~ 3.7 Ga that could be associated with formation of the overlapping large crater, the Rheasilvia basin. Multispectral images from the NASA Dawn Mission have revealed signatures suggestive of diogenite-rich material within the Rheasilvia basin (Reddy et al., 2012) indicating material was excavated down to the upper mantle by the impact.

Scenario (2): the ~ 3.7 Ga age could be related to the Veneneia Basin feature, while the origin of the Lake Carnegie sample impact site is now obscured by later resurfacing of the asteroid. Secondly, Millbillillie with an age of 3313 ± 174 Ma is suggested to represent resetting of the K/Ar system during a later small impact that reset pyroxene ages. This impact is inferred to be too small to be related to any major impact structures recorded by 4 Vesta. Importantly, in most published age data (e.g., Bogard and Garrison, 2003), either robust or perturbed, there is no sign of

any major thermal event as young as 1 Ga that would support this as an age for the formation of the vestoid family (Marzari et al., 1996; Marchi et al., 2012; Schenk et al., 2012).

5.5. Significances of the cosmic ray exposure ages

CRE ages for the five meteorites studied here range from ~ 6 to ≥ 40 Ma (Table 3). However it should be kept in mind that depth of burial within the meteoroid influences the results obtained via the production rate of cosmogenic ^{38}Ar . Hence, CRE ages should be considered as approximate (minimum) ages only. In addition, if the meteorite was located close to the surface of its parent body before ejection, then the $^{38}\text{Ar}_c$ age represents the time since ejection, plus the time at the surface of the parent body.

The CRE age for Camel Donga was ~ 40 Ma and Millbillillie gave two ages with robust P -values (18 ± 1 Ma and 17 ± 2 Ma) from which a weighted mean value of 17.8 ± 0.9 Ma (MSWD = 1.6; $P = 0.2$) could be calculated. Lake Carnegie resulted in a weighted mean value of 6.1 ± 0.9 Ma (MSWD = 0.4; $P = 0.53$) and only one CRE age with a robust P -value: 15 ± 1 Ma was obtained from Deakin 010. No weighted mean value could be calculated for Old Homestead 003 as there was insufficient spread along the cosmochron. These ages imply that either the meteorites were released from the HED parent body at the minimum impact age recorded in this study and that they subsequently resided in a parent meteoroid shielded at depth from cosmic rays until released by further small impact events or that they were released from the parent body at their CRE ages and exposed to cosmic rays until entry to Earth. We favour the first interpretation as there is no evidence for impact age resetting coinciding with the CRE ages as would be expected from an impact large enough to excavate the material from its parent body. As pre-

viously mentioned the petrologic features of Lake Carnegie, such as equilibration of pyroxenes, coarse-grain size and lack of brecciation, suggest that this sample was excavated from a considerable depth early in the formation history of the HED parent body. If this is correct the sample must have resided inside a large meteoroid, at least a few metres below the surface, before its arrival on Earth.

The two weighted mean CRE ages from this study: Millbillillie (CRE = 17.8 ± 0.9 Ma) and Lake Carnegie (CRE = 6.1 ± 0.9 Ma) lie within two of Eugster and Michel's (1995) five groups that include 81% of CRE ages for HEDs: 6 ± 1 Ma and 21 ± 4 Ma.

6. CONCLUSIONS

New robust $^{40}\text{Ar}/^{39}\text{Ar}$ plateau ages allow us to reach the following conclusions:

1. The $^{40}\text{Ar}/^{39}\text{Ar}$ plateau ages obtained for the Lake Carnegie cumulate eucrite (weighted mean age of 4507 ± 20 Ma) record a major thermal event within $\sim 60 \pm 20$ Ma of the beginning of the differentiation of the HED parent body. This ~ 4.51 Ga age could: (1) reflect a cooling age of the surface or external portion of the asteroid as supported by the absence of shock features in the different mineral phases; or (2) record the mega-impact that ejected a major chunk of the asteroid. We consider the mega-impact scenario to be most likely, based on the lack of evidence for subsequent resetting of the K/Ar system in most of the unbreciated eucrites, and the apparent synchronicity between all available plateau ages recorded by the ~ 4.5 Ga eucrites. Assuming a mega-impact scenario to be correct this might indicate that Lake Carnegie was excavated at ~ 4.51 Ga, possibly from the south polar Veneneia basin that underlies the younger Rheasilvia impact basin.
2. If it is correct than there has been no magmatism post ~ 4.4 Ga in the HED source body then three separate impact events are recorded by a single meteorite (Millbillillie). Careful separation and analysis of three phases resulted in plateau ages of 3722 ± 55 Ma (plagioclase), 3579 ± 28 Ma (matrix), and 3313 ± 174 Ma (pyroxene and matrix). These ages correspond to three different time/temperature histories that are likely related to the size of impact events: (i) large: recorded by plagioclase; (ii) intermediate: recorded by the matrix; and (iii) small recorded by pyroxene.
3. Camel Donga and Millbillillie record a temporal evolution of large to small impacts that range from 3722 ± 55 Ma to 3313 ± 174 Ma. The ages of the largest impacts seem to cluster between ~ 3.8 and ~ 3.5 Ga suggesting that the duration of the main phase of bombardment on the HED parent body(ies) might be shorter than previously thought, but is still relatively unconstrained at this stage. Additional high quality plateau ages are required to constrain the duration of the bombardment of the HED parent body more precisely.
4. Plateau ages show a small cluster of ages around ~ 3.7 Ga that could be associated with formation of the younger Rheasilvia basin. Alternatively, although per-

haps less likely, the ~ 3.7 Ga ages may correlate with the Veneneia basin, in this scenario our interpretation that the Lake Carnegie mega-impact excavated the Rheasilvia basin is incorrect. In which case visual evidence of a Lake Carnegie mega-impact on 4 Vesta is long gone and the material that had been excavated by formation of the Rheasilvia basin has not been sampled by the HED meteorite collection recovered on Earth.

5. CRE ages for the five meteorites studied here range from ~ 6 to 40 Ma. The relatively young CRE ages of these meteorites, compared to the $^{40}\text{Ar}/^{39}\text{Ar}$ ages, indicate that the impacts that released them from their parent body(s) or host meteoroid(s) did not reset the older impact event ages recorded by the K/Ar system.

ACKNOWLEDGMENTS

Peter Downes is thanked for early SEM work. We also thank D. Bogard, G. Herzog, J. Levine and one anonymous reviewer for very thoughtful, detailed, and constructive reviews which have greatly improved this manuscript. T.K. was supported by an Australian Postgraduate Award and a University of Western Australia Top Up Scholarship during this research.

APPENDIX A. SUPPLEMENTARY DATA

Supplementary data associated with this article can be found, in the online version, at <http://dx.doi.org/10.1016/j.gca.2013.03.040>.

REFERENCES

- Allègre C. J., Birck J. L., Fourcade S. and Semet M. P. (1975) Rubidium-87/Strontium-87 age of Juvinas basaltic achondrite and early igneous activity in the solar system. *Science* **187**, 436–438.
- Amelin Y. (2008) The U-Pb systematics of angrite Sahara 99555. *Geochim. Cosmochim. Acta* **72**, 4874–4885.
- Baksi A. K. (2007) A quantitative tool for evaluating alteration in undisturbed rocks and minerals – I: water, chemical weathering and atmospheric argon. In *The Origin of Melting Anomalies, Plates, Plumes and Planetary Processes* (eds. G. R. Foulger and D. M. Jurdy). *Geol. Soc. Amer. Spec. Paper* **430**. pp. 285–308.
- Binzel R. P. and Xu S. (1993) Chips off of asteroid 4 Vesta: evidence for the parent body of basaltic achondrite meteorites. *Science* **260**, 186–191.
- Binzel R. P., Gaffey M. J., Thomas P. C., Zellner B. H., Storrs A. D. and Wells E. N. (1997) Geologic mapping of Vesta from 1994 Hubble Space Telescope images. *Icarus* **128**, 95–103.
- Bland P. A., Spurny P., Towner M. C., Bevan A. W. R., Singleton A. T., Bottke, Jr., W. F., Greenwood R. C., Chesley S. R., Šrbený L., Borovička J., Ceplecha Z., McCafferty T. P., Vaughan D., Benedix G. K., Deacon G., Howard K. T., Franchi I. A. and Hough R. M. (2009) An anomalous basaltic meteorite from the innermost main belt. *Science* **325**, 1525–1527.
- Bogard D. D. (1995) Impact ages of meteorites: a synthesis. *Meteoritics* **30**, 244–268.
- Bogard D. D. (2011) K-Ar ages of meteorites: clues to parent-body thermal histories. *Chem. Erde* **71**, 207–226.

- Bogard D. D. and Garrison D. H. (2003) ^{39}Ar – ^{40}Ar ages of eucrites and thermal history of asteroid 4 Vesta. *Meteorit. Planet. Sci.* **38**, 669–710.
- Buchanan P. C., Noguchi T., Bogard D. D., Ebihara M. and Katayama I. (2005) Glass veins in the unequilibrated eucrite Yamato 82202. *Geochim. Cosmochim. Acta* **69**, 1883–1898.
- Burbine T. H., Meibom A. and Binzel R. P. (1996) Mantle material in the main belt: battered to bits? *Meteorit. Planet. Sci.* **31**, 607–620.
- Carlson R. W. and Lugmair G. W. (2000) Timescales of planetesimal formation and differentiation based on extinct and extant radioisotopes. In *Origin of the Earth and Moon* (eds. R. M. Canup and K. Righter). Univ. Arizona Press and Lunar Planet. Inst., Houston, pp. 25–44.
- Cassata W. S., Renne P. R. and Shuster D. L. (2009) Argon diffusion in plagioclase and implications for thermochronometry: a case study from the Bushveld Complex, South Africa. *Geochim. Cosmochim. Acta* **73**, 6600–6612.
- Cassata W. S., Shuster D. L., Renne P. R. and Weiss B. P. (2010) Evidence for shock heating and constraints on Martian surface temperatures revealed by ^{40}Ar / ^{39}Ar thermochronometry of Martian meteorites. *Geochim. Cosmochim. Acta* **74**, 6900–6920.
- Cassata W. S., Renne P. R. and Shuster D. L. (2011) Argon diffusion in pyroxenes: implications for thermochronometry and mantle degassing. *Earth Planet. Sci. Lett.* **304**, 407–416.
- Clayton R. N. and Mayeda T. K. (1996) Oxygen isotope studies of achondrites. *Geochim. Cosmochim. Acta* **60**, 1999–2017.
- Consolmagno G. J. and Drake M. J. (1977) Composition and evolution of the eucrite parent body: evidence from rare earth elements. *Geochim. Cosmochim. Acta* **41**, 1271–1282.
- Cruikshank D. P., Tholen D. J., Hartmann W. K., Bell J. F. and Brown R. H. (1991) Three basaltic earth-approaching asteroids and the source of the basaltic meteorites. *Icarus* **89**, 1–13.
- Eugster O. and Michel Th. (1995) Common asteroid break-up events of eucrites, diogenites, and howardites and cosmic-ray production rates for noble gases in achondrites. *Geochim. Cosmochim. Acta* **59**, 177–199.
- Gaffey M. J. (1997) Surface lithologic heterogeneity of asteroid 4 Vesta. *Icarus* **127**, 130–157.
- Ghosh A. and McSween, Jr., H. Y. (1998) A thermal model for the differentiation of asteroid 4 Vesta, based on radiogenic heating. *Icarus* **134**, 187–206.
- Gomes R., Levison H. F., Tsiganis K. and Morbidelli A. (2005) Origin of the cataclysmic Late Heavy Bombardment period of the terrestrial planets. *Nature Lett.* **435**, 466–469.
- Hennessy J. and Turner G. (1980) ^{40}Ar – ^{39}Ar ages and irradiation history of luna 24 basalts. *Phil. Trans. Roy. Soc. London Ser. A, Math. Phys. Sci.* **297**(1428), 27–39.
- Jourdan F. (2012) The ^{40}Ar / ^{39}Ar dating technique applied to planetary sciences and terrestrial impacts. *Aust. J. Earth Sci.* **59**, 199–224.
- Jourdan F. and Renne P. R. (2007) Age calibration of the Fish Canyon sanidine ^{40}Ar / ^{39}Ar dating standard using primary K–Ar standards. *Geochim. Cosmochim. Acta* **71**, 387–402.
- Jourdan F., Renne P. R. and Reimold W. U. (2009) An appraisal of the ages of terrestrial impact structures. *Earth Planet. Sci. Lett.* **286**, 1–13.
- Jourdan F., Bland P. A., Bouvier A. and Benedix G. (2011) A ~3.63 Ga major impact recorded by the Bunburra Rockhole anomalous basaltic achondrite. *Mineral. Mag.* **75**, 1128.
- Kaneoka I., Nagao K., Yamaguchi A. and Takeda H. (1995) ^{40}Ar / ^{39}Ar Analyses of Juvinas Fragments. *Proc. NIPR Symp. Antarct. Meteorit.* **8**, 287–296.
- Kleine T., Münker C., Mezger K. and Palme H. (2002) Rapid accretion and early core formation on asteroids and the terrestrial planets from Hf–W chronometry. *Nature* **418**, 952–955.
- Koppers A. A. P. (2002) ArArCALC-software for ^{40}Ar / ^{39}Ar age calculations. *Comput. Geosci.* **28**, 605–619.
- Korochantseva E. V., Trieloff M., Buikin A. I., Hopp J. and Meyer H.-P. (2005) ^{40}Ar – ^{39}Ar dating and cosmic-ray exposure time of desert meteorites: Dhofar 300 and Dhofar 007 eucrites and anomalous achondrite NWA 011. *Meteorit. Planet. Sci.* **40**, 1433–1454.
- Kunz J., Falter M. and Jessberger E. K. (1997) Shocked meteorites: Argon-40-argon-39 evidence for multiple impacts. *Meteorit. Planet. Sci.* **32**, 647–670.
- Lentz R. C. F., Scott E. R. D. and McCoy T. J. (2007) Anomalous eucrites: using Fe/Mn to search for different parent bodies. *Lunar Planet. Sci.* **38**. Lunar Planet. Inst., Houston. #1968 (abstr.).
- Levine J., Renne P. R. and Muller R. A. (2007) Solar and cosmogenic argon in dated lunar impact spherules. *Geochim. Cosmochim. Acta* **71**, 1624–1635.
- Lugmair G. W. and Shukolyukov A. (1998) Early solar system timescales according to ^{53}Mn – ^{53}Cr systematics. *Geochim. Cosmochim. Acta* **62**, 2863–2886.
- Mahon K. I. (1996) The NEW “York” regression: application of an improved statistical method to geochemistry. *Int. Geol. Rev.* **38**, 293–303.
- Marchi S., McSween H. Y., O’Brien D. P., Schenk P., De Sanctis M. C., Gaskell R., Jaumann R., Mottola S., Preusker F., Raymond C. A., Roatsch T. and Russell C. T. (2012) The violent collisional history of asteroid 4 Vesta. *Science* **336**, 690–694.
- Marzari F., Cellino A., Davis D. R., Farinella P., Zappala V. and Vanzani V. (1996) Origin and evolution of the Vesta asteroid family. *Astron. Astrophys.* **316**, 248–262.
- McCord T. B., Adams J. B. and Johnson T. V. (1970) Asteroid Vesta: spectral reflectivity and compositional implications. *Science* **168**, 1445–1447.
- McDougall I. and Harrison T. M. (1999) *Geochronology and Thermochronology by the ^{40}Ar / ^{39}Ar Method*. Oxford Univ. Press, Oxford, p. 269.
- McEwen A. S. and Bierhaus E. B. (2006) The importance of secondary cratering to age constraints on planetary surfaces. *Annu. Rev. Earth Planet. Sci.* **34**, 535–567.
- Mittlefehldt D. W. (2005) Ibitira: a basaltic achondrite from a distinct parent asteroid and implications for the Dawn mission. *Meteorit. Planet. Sci.* **40**, 665–677.
- Mittlefehldt D. W., McCoy T. J., Goodrich C. A. and Kracher A. (1998) Non-chondritic meteorites from asteroidal bodies. In *Planetary Materials, Reviews in Mineralogy*, vol. 36 (ed. J. J. Papike). Min. Soc. Amer., pp. 4–2–4–195.
- Miyamoto M. and Takeda H. (1994) Evidence for excavation of deep crustal material of a Vesta-body from Ca compositional gradients in pyroxene. *Earth Planet. Sci. Lett.* **122**, 343–349.
- Moskovitz N. A., Jedicke R., Gaidos E., Willman M., Nesvorný D., Fevig R. and Ivezić Z. (2008) The distribution of basaltic asteroids in the Main Belt. *Icarus* **198**, 77–90.
- NASA Dawn Mission. (2011) <<http://dawn.jpl.nasa.gov/multimedia/imageoftheday/archives.asp?month=2011-September>>.
- Niemeyer S. and Leich D. A. (1976) Atmospheric rare gases in lunar rock 60015. *Proc. Lunar Sci. Conf.* 7th. pp. 587–597.
- Nyquist L. E., Takeda H., Bansal B. M., Shih C.-Y., Wiesmann H. and Wooden J. L. (1986) Rb–Sr and Sm–Nd internal isochron ages of subophitic basalt clast and a matrix sample from the Y75011 eucrite. *J. Geophys. Res.* **91**, 8137–8150.
- Nyquist L., Bogard D., Takeda H., Bansal B., Wiesmann H. and Shih C.-Y. (1997) Crystallization, recrystallization and impact-

- metamorphic ages of eucrites Y792510 and Y791186. *Geochim. Cosmochim. Acta* **61**, 2119–2132.
- O'Brien D. P., Marchi S., Schenk P., Mittlefehldt D. W., Jaumann R., Ammannito E., Buczkowski D. L., De Sanctis M. C., Filacchione G., Gaskell R., Hoffmann M., Joy S., LeCorre L., Li J.-Y., Nathues A., Polanskey C., Preusker F., Rayman M., Raymond C. A., Reddy V., Roatsch T., Russell C. T., Turrini D., Vincent J.-B., and the Dawn Science Team (2012) The impact history of Vesta: new views from the Dawn Mission. *Lunar Planet. Sci.* **43**. Lunar Planet. Inst., Houston. #4031(abstr.).
- Palme H., Wlotzka F., Spettel B., Dreibus G. and Weber H. (1988) Camel Donga: a eucrite with high metal content. *Meteoritics* **23**, 49–57.
- Reddy V., Nathues A., Le Corre L., Sierks H., Li J.-Y., Gaskell R., McCoy T., Beck A. W., Schröder S. E., Pieters C. M., Becker K. J., Burrati B. J., Denevi B., Blewett D. T., Christensen U., Gaffey M., Gutierrez-Marques P., Hicks M., Keller H. U., Maue T., Mottola S., McFadden L. A., McSween H. Y., Mittelfeildt D., O'Brien D. P., Raymond C. and Russell C. (2012) Color and albedo heterogeneity of Vesta from Dawn. *Science* **336**, 700–704.
- Renne P. R., Swisher C. C., Deino A. L., Karner D. B., Owens T. L. and De Paolo D. J. (1998) Intercalibration of standards, absolute ages and uncertainties in $^{40}\text{Ar}/^{39}\text{Ar}$ dating. *Chem. Geol.* **145**, 117–152.
- Renne P. R., Mundil R., Balco G., Min K. and Ludwig K. R. (2010) Joint determination of ^{40}K decay constants and $^{40}\text{Ar}^*/^{40}\text{K}$ for the Fish Canyon sanidine standard, and improved accuracy for $^{40}\text{Ar}/^{39}\text{Ar}$ geochronology. *Geochim. Cosmochim. Acta* **74**, 5349–5367.
- Schenk P., O'Brien D. P., Marchi S., Gaskell R., Preusker F., Roatsch T., Jaumann R., Buczkowski D., McCord T., McSween H. Y., Williams D., Yingst A., Raymond C. and Russell C. (2012) The geologically recent giant impact basins at Vesta's South Pole. *Science* **336**, 694–697.
- Shuster D. L., Balco G., Cassata W. S., Fernandes V. A., Garrick-Bethell I. and Weiss B. P. (2010) A record of impacts preserved in the lunar regolith. *Earth Planet. Sci. Lett.* **290**, 155–165.
- Scott E. R. D., Greenwood R. C., Franchi I. A. and Sanders I. S. (2009) Oxygen isotopic constraints on the origin and parent bodies of eucrites, diogenites, and howardites. *Geochim. Cosmochim. Acta* **73**, 5835–5853.
- Shukolyukov A. and Lugmair G. W. (1993) ^{60}Fe in eucrites. *Earth Planet. Sci. Lett.* **119**, 159–166.
- Smoliar M. I. (1993) A survey of Rb-Sr systematic of eucrites. *Meteorit. Planet. Sci.* **28**, 105–113.
- Srinivasan G., Goswami J. N. and Bhandari N. (1999) ^{26}Al in eucrite Piplia Kalan: plausible heat source and formation chronology. *Science* **284**, 1348–1350.
- Steiger R. H. and Jäger E. (1977) Subcommission on geochronology: convention on the use of decay constants in geo- and cosmochronology. *Earth Planet. Sci. Lett.* **36**, 359–362.
- Takeda H. and Graham A. L. (1991) Degree of equilibration of eucritic pyroxenes and thermal metamorphism of the earliest planetary crust. *Meteoritics* **26**, 129–134.
- Tera F., Carlson R. W. and Boctor N. Z. (1997) Radiometric ages of basaltic achondrites and their relation to the early history of the Solar System. *Geochim. Cosmochim. Acta* **61**, 1713–1731.
- Vilas F., Cochran A. L. and Jarvis K. S. (2000) Vesta and the Vestoids: a new rock group? *Icarus* **147**, 119–128.
- Wadhwa M., Srinivasan G. and Carlson R. W. (2006) Timescales of planetesimal differentiation in the early Solar System. In *Meteorites and the Early Solar System II* (eds. D. S. Lauretta and H. Y. McSween Jr.). The Uni. Arizona Press in collaboration with Lunar Planet. Inst. pp. 715–731.
- Wadhwa M., Amelin Y., Bogdanovski O., Shukolyukov A., Lugmair G. W. and Janney P. (2009) Ancient relative and absolute ages for a basaltic meteorite: implications for timescales of planetesimal accretion and differentiation. *Geochim. Cosmochim. Acta* **73**, 5189–5201.
- Wasson J. T. and Chapman C. R. (1996) Space weathering of basalt-covered asteroids: Vesta an unlikely source of the HED meteorites (abstract). In *Workshop on Evolution of Igneous Asteroids: Focus on Vesta and the HED Meteorites*. LPI Technical Report 96-02, Part 1. Lunar Planet. Inst., Houston. pp 38–39.
- Wiechert U. H., Halliday A. N., Palme H. and Rumble D. (2004) Oxygen isotope evidence for rapid mixing of the HED meteorite parent body. *Earth Planet. Sci. Lett.* **221**, 373–382.
- Yamaguchi A., Takeda H., Bogard D. D. and Garrison D. H. (1994) Textural variation and impact of the Millbillillie eucrite. *Meteoritics* **29**, 237–245.
- Yamaguchi A., Taylor G. J. and Keil K. (1996) Global crustal metamorphism of the eucrite parent body. *Icarus* **124**, 97–112.
- Yamaguchi A., Taylor G. J. and Keil K. (1997) Metamorphic history of the eucritic crust of 4 Vesta. *J. Geophys. Res.* **102**, 13381–13386.
- Yamaguchi A., Taylor G. J., Keil K., Floss C., Crozaz G., Nyquist L. E., Bogard D. D., Garrison D. H., Reese Y. D., Wiesmann H. and Shih C.-Y. (2001) Post-crystallization reheating and partial melting of eucrite EET90020 by impact into the hot crust of asteroid 4 Vesta ~4.5 Ga ago. *Geochim. Cosmochim. Acta* **65**, 3577–3599.
- Yamaguchi A., Clayton R. N., Mayeda T. K., Ebihara M., Oura Y., Miura Y. N., Haramura H., Misawa K., Kojima H. and Nagao K. (2002) A new source of basaltic meteorites inferred from northwest Africa 001. *Science* **296**, 334–336.

Associate editor: Gregory F. Herzog